isvr Institute of Sound and Vibration Research

Dynamic Behaviour and Transmission Characteristics of Structure-Borne Noise of Marine Diesel Engine Generator with Resilient Rubber Mounts and Elastic Foundation

D.C. Lee, M.J. Brennan and B.R. Mace

ISVR Technical Memorandum No 943

December 2004

University of Southampton

SCIENTIFIC PUBLICATIONS BY THE ISVR

Technical Reports are published to promote timely dissemination of research results by ISVR personnel. This medium permits more detailed presentation than is usually acceptable for scientific journals. Responsibility for both the content and any opinions expressed rests entirely with the author(s).

Technical Memoranda are produced to enable the early or preliminary release of information by ISVR personnel where such release is deemed to the appropriate. Information contained in these memoranda may be incomplete, or form part of a continuing programme; this should be borne in mind when using or quoting from these documents.

Contract Reports are produced to record the results of scientific work carried out for sponsors, under contract. The ISVR treats these reports as confidential to sponsors and does not make them available for general circulation. Individual sponsors may, however, authorize subsequent release of the material.

UNIVERSITY OF SOUTHAMPTON

INSTITUTE OF SOUND AND VIBRATION RESEARCH

DYNAMICS GROUP

Dynamic Behaviour and Transmission Characteristics of Structure-Borne Noise of Marine Diesel Engine Generator with Resilient Rubber Mounts and Elastic Foundation

by

D.C. Lee, M.J. Brennan and B.R. Mace

ISVR Technical Memorandum No: 943

December 2004

Authorised for issue by
Professor M.J. Brennan
Group Chairman

Contents

Abstract

Vibration and noise isolation using resilient rubber mounts on a marine diesel engine is a well-known and popular technique. Even though it is a general method, its practical application is more complex. The resilient mounts of a diesel engine installed onboard a ship should be designed for both static and dynamic loads. In particular, if possible, the major resonances of the six rigid body modes of the installation and the flexible modes of the engine structure should be avoided within the engine operation range. In this report, a diesel engine generator in the 5500 TEU container vessel which had an elastic foundation was selected as a theoretical and test model. The dynamic behaviour and the transmission of structure-borne noise are investigated by theoretical and experimental methods and these are verified by vibration tests onboard. The theoretical analysis of the test model was performed by using a single mass 6 degree of freedom system. Actual measurements of mechanical vibration of the engine and its foundation onboard were carried out to test the modeling approach.

The design criteria in vibration of marine diesel engines may be stated in terms of the vibration. Even though this method is generally used, it cannot be used to fully evaluate the optimum design in marine diesel engines with resilient mounting systems. A complementary method is proposed which can estimate the vibration by the summation of dynamic force transmitted through the resilient mounts. Furthermore in order to reduce the structure-borne noise transmitted to the engine foundation, the vertical vibration resonance frequencies of the foundation should not coincide with the rotational motion of the engine excited by 0.5^{th}, 1^{st}, 1.5^{th}, 2^{nd} ... times the engine cylinder number at the synchronous speed of the generator.

1. INTRODUCTION

1.1 Introduction

Vibration and noise isolation using resilient rubber mounts on a marine diesel engine is a well-known and popular technique. Even though it is a general method, its practical application is more complex. The resilient mounts of a diesel engine installed onboard a ship of shipboard should be designed for both static and dynamic loads. The static design is governed by its weight, the mean torque transmitted to the generator and the seaway movement caused by rolling and pitching motion of the ship. The dynamic design criteria are governed by the 1st and 2nd unbalance moments, H-type and X-type guide force moments (see Fig 11) originating from the reciprocating and rotating mass of the piston and combustion gas pressure within the cylinders. The major resonances of the six rigid body modes of the installation and the flexible modes of its support structure, should be avoided within the engine operation range. In this report, a diesel engine generator in a 5500 TEU container vessel which could not avoid exciting the elastic effects of the foundation was selected as a case study & test model. The dynamic behaviour of the system and transmission of structure-borne noise into the foundation are investigated theoretically and are verified by vibration tests onboard. An evaluation method for the optimum design of a resilient mounting system based on actual service experience is proposed.

1.2 Literature review

Marine diesel engine generators have been directly fixed to the hulls of general ships with the exception of luxury ships until the middle of 1990's. Since then, the use of resilient mounts between the diesel engine and the hull to isolate or reduce vibration and noise has increased steadily by the requirement placed on ship owners to provide a comfortable life onboard. The optimum design and application of a large resilient mount system which has to support a heavy load such as a marine diesel engines were mainly conduced by the mount manufacturers [1] and

large diesel engine manufacturers [2,3]. The optimum design and study of hydro-mount systems for automobiles was performed by Royston and Singh [4]. Academic studies of resilient mounts including marine engine mount systems were performed by Lee et al [5] and Tao et al[6]. The effect of the elastic foundation on the dynamic response of an engine mount system in automobiles was evaluated by Kim and Lee [7]. Also, the flexible effect of the foundation in a supercritical rotor was evaluated by Bonello and Brennan [8]. However, the optimum design of a marine diesel engine generator with resilient mount system should be performed with cost in mind so that its application can be realised in practice.

1.3 Outline of report

The main body of this report consists of five sections. Following the introduction in section 1, the theoretical analysis method for marine diesel engine generators with resilient mounts is introduced in section 2. Additionally, the dynamic characteristics of resilient rubber mounts are introduced. Also, the elastic effect in the vertical direction of the engine foundation is combined with the stiffness of the resilient mount. A resiliently supported rigid body model is analyzed by a 6 degree of freedom model. An evaluation method for the design of mounting systems with regard to the mechanical vibration of marine diesel engine generators is additionally proposed.

In section 3 the natural frequencies and free vibration modes without damping are considered the theoretical analysis of forced vibration of the cylinders under normal firing condition, and with uneven firing and forced vibration with one cylinder misfiring, is also considered. In section 4 the analytical results performed in section 3 are compared with experimental results onboard. Finally, conclusions are drawn in section 5.

2. THEORETICAL VIBRATION ANALYSIS OF MARINE DIESEL ENGINE GENERATOR WITH RESILIENT MOUNT

2.1 Dynamic characteristics of resilient rubber mount

In this study, a resilient mount for a marine diesel engine is considered to be made from rubber with a conical shape and cross section as shown in figure 1. The dynamic behaviour of resilient rubber mounts for vibration isolation is not simple. The measurement methods of vibro-acoustic transfer properties of resilient elements in the laboratory for vibration analysis are recommended by the ISO [9~11]. The dynamic stiffness and acoustic properties of the mount shown in figure 1 were measured by its manufacturer [1,12]. The transfer-functions in the vertical and horizontal direction of the RD-214 [12] with shore grade 55, with static preload of 49 kN applied, are shown in figure 2. In figure 3 the same results are represented as stiffness curves which are calculated by multiplying the transfer-function by $\omega^2 (= (2\pi f)^2)$. Where f is the excitation frequency in Hz. The input impedance of the mount can be estimated by the transfer impedance "Z" which can be calculated from the mounting transfer function "T", by

$$|Z| = |T| \cdot \omega \qquad (2.1)$$

A reasonable impedance mismatch should be designed and achieved in the foundation of a marine diesel engine generator. As an example, the impedance of mountings with shore grade 65 and the foundation including the hull is shown in figure 4. It is important to consider how to install many mounts, what the interval should be between the mounts, and how to select stiffness. The major resonances of the foundation of marine diesel engine generator should also be avoided by the engine excitation in the view of structure-borne noise transmission. The interference between the mounts can be written as a function of Helmholtz number shown by

$$K_X = 2\pi \cdot \frac{x}{\lambda_p} \tag{2.2}$$

where K_X is the Helmholz number, x is the distance between each resilient mount [m] and λ_p is the bending wave length in the foundation. At high frequencies the wave length will be short and as a consequence the Helmholz number large and vice versa at low frequencies. The results are presented for K_X= 0.01 to K_X= 10 which is relevant for most applications with a frequency range of 10 to 10000 Hz.

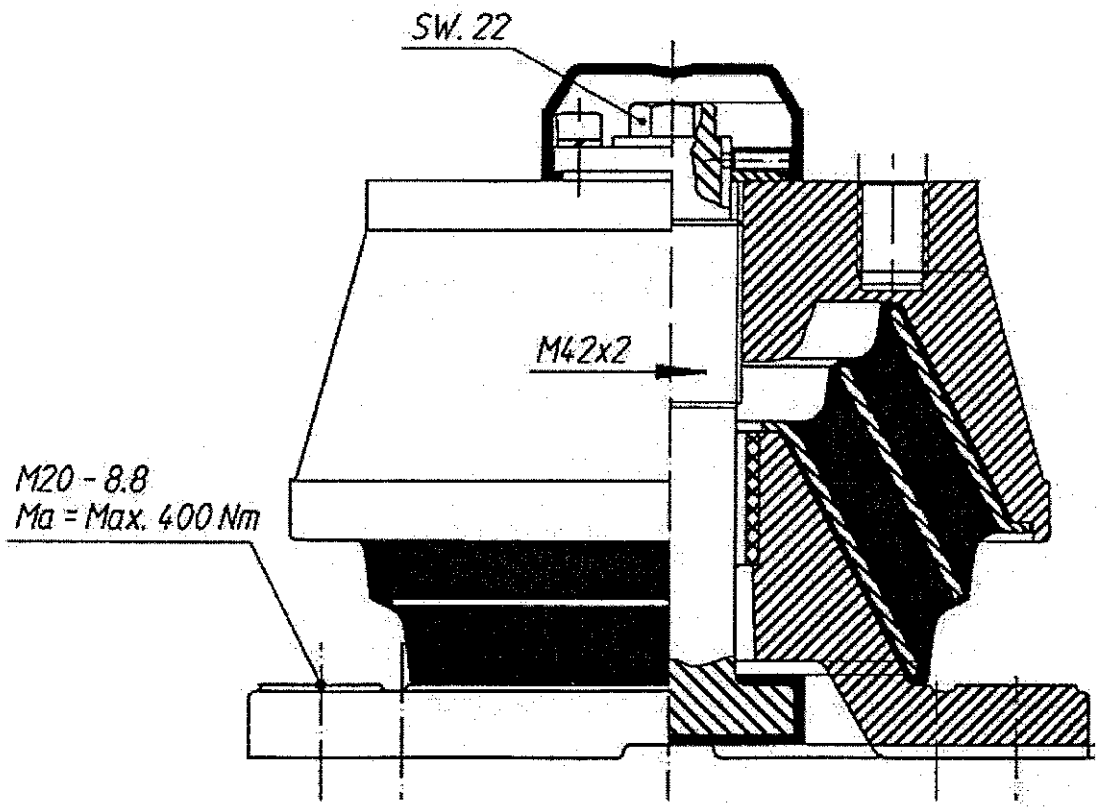

Figure 1. The section view of RD-214-55[12] conical resilient mount of rubber type

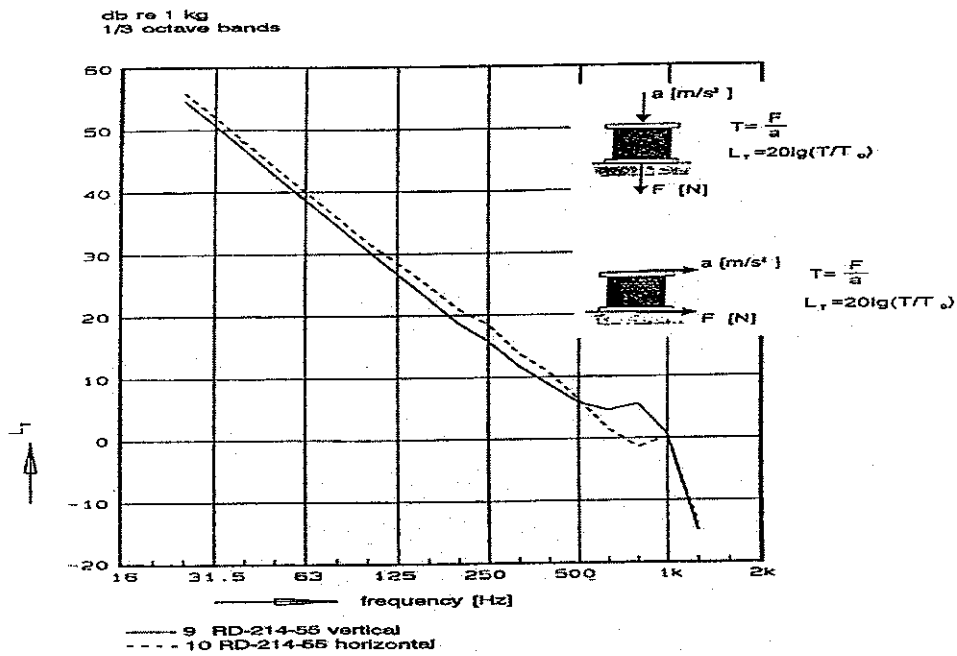

Figure 2. The transfer function/T in the vertical and the horizontal direction of resilient mount RD-214-55

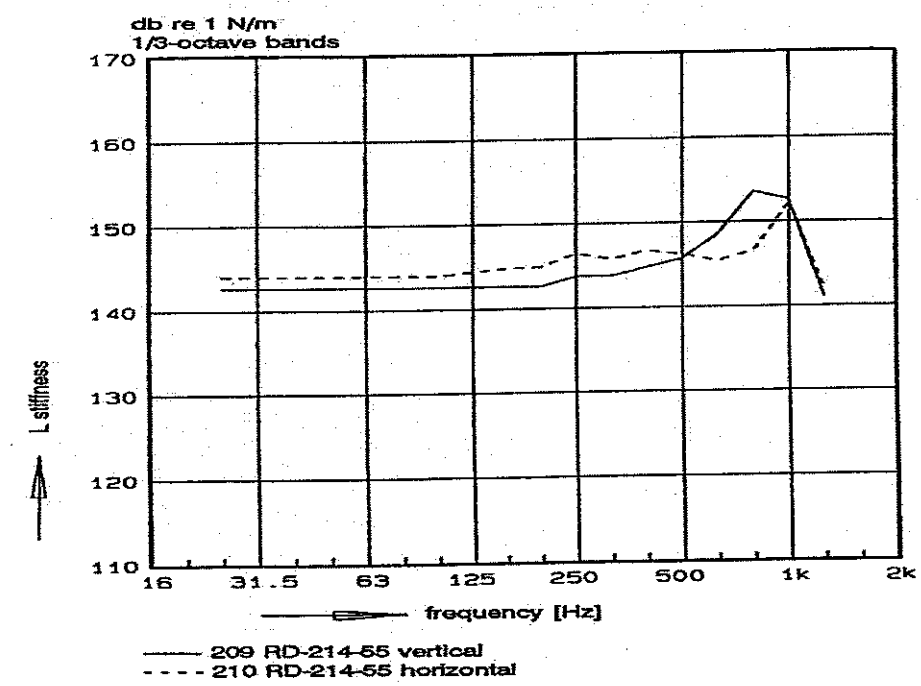

Figure 3. The stiffness in the vertical and the horizontal direction of resilient mount RD-214-55

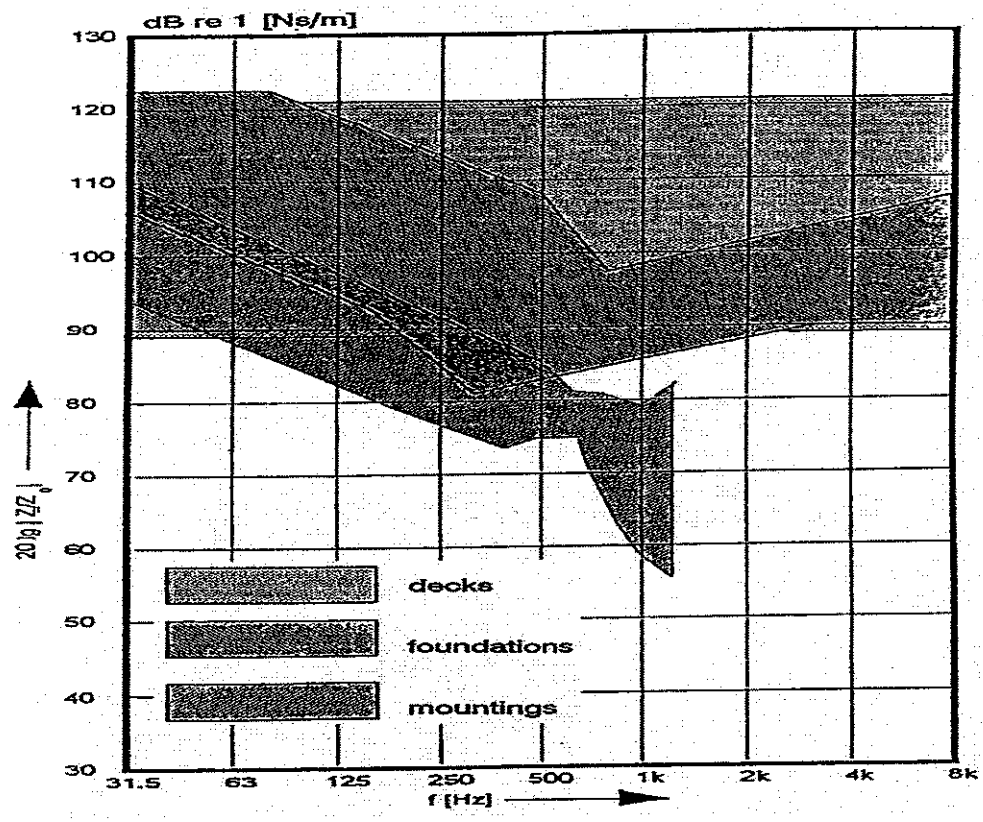

Figure 4. The impedance area of mountings with shore grade 65 and hull foundation [1]

2.2 Elastic effect in engine foundation

The ideal foundation for a marine diesel engine generator is a rigid structure which can sufficiently withstand the static and dynamic loads. However, it is difficult to realise a stiff structure in a ship, because the design of the hull structure must be cost effective, so the engine foundation is an elastic structure. In this report, the vertical flexibility of test model used in section 3 and 4 was investigated using experimental methods [13,14]. It is composed of two symmetrical foundations which can support resilient mounts of 6 units on the right-hand and left-hand side respectively. The vertical vibration mode of this structure is very important in the transmission characteristics of structure-borne noise. Figures 5~8 show the results that were

measured by a hammer test onboard. Even though the vibration test result has some uncertain factors, it can be used to understand easily the transmission characteristics of structure-borne noise in section 4. Table 1 shows the resonances of the vertical foundation for experimental results shown in Figure 5~8. Acceleration amplitudes at frequencies less than 150 Hz(high pass filter) and more than frequency 250 Hz(low pass filter) can be neglected as the have small values. Table 2 shows the stiffness of the vertical foundation which was calculated by the experimental lower resonance and equivalence mass. The stiffness of the resilient mount used in these calculations is shown in figure 3.

Table 1 Resonances of vertical direction of engine foundation for 9L28/32 engine generator of 5500 TEU container vessel (Hz)

No.	Measurement (R1 point)	Measurement (R4 point)	Measurement (R5 point)	Measurement (R6 point)
1	117.5	121.3	123.8	-
2	136.3	133.8	-	-
3	158.8	158.8	158.8	157.5
4	176.3	176.3	-	173.8
5	211.3	210.0	206.0	203.8
6	-	233.8	-	222.5

Table 2 Dynamic stiffness of engine foundation and resilient mount type RD 214-55 for 9L28/32 engine generator of 5500 TEU container vessel (Unit : MN/m)

Direction	Engine foundation(s_1)	Resilient mount(s_2)	Ratio(S_1/S_2)
x(axial)	Rigid(Large)	8.75	-
y(transverse)	Rigid(Large)	8.75	-
z(vertical)	119.6 within ± 20%	7.14	16.75

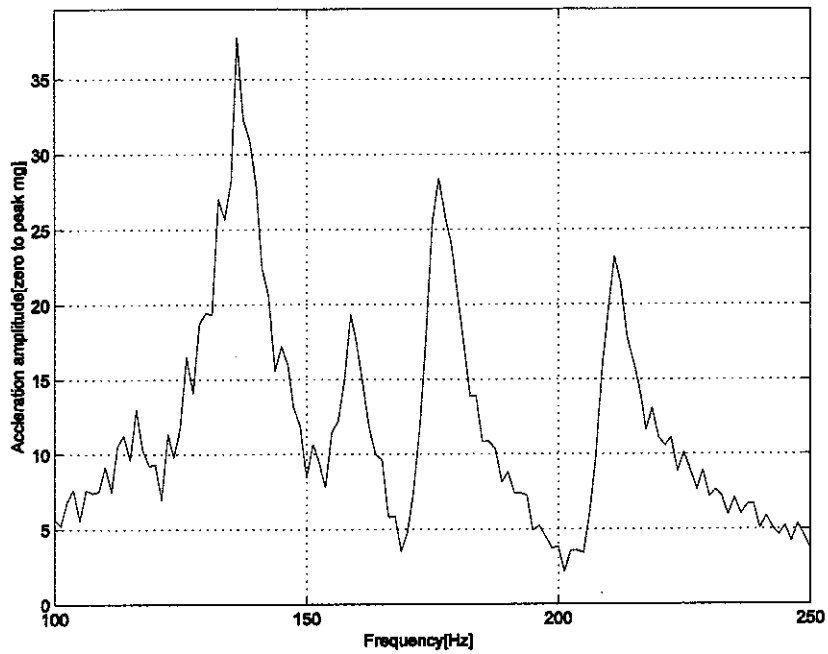

Figure 5. The measured vertical vibration of engine foundation of 9L28/32 generator engine of 5500 TEU container vessel at resilient mount right No.1 position

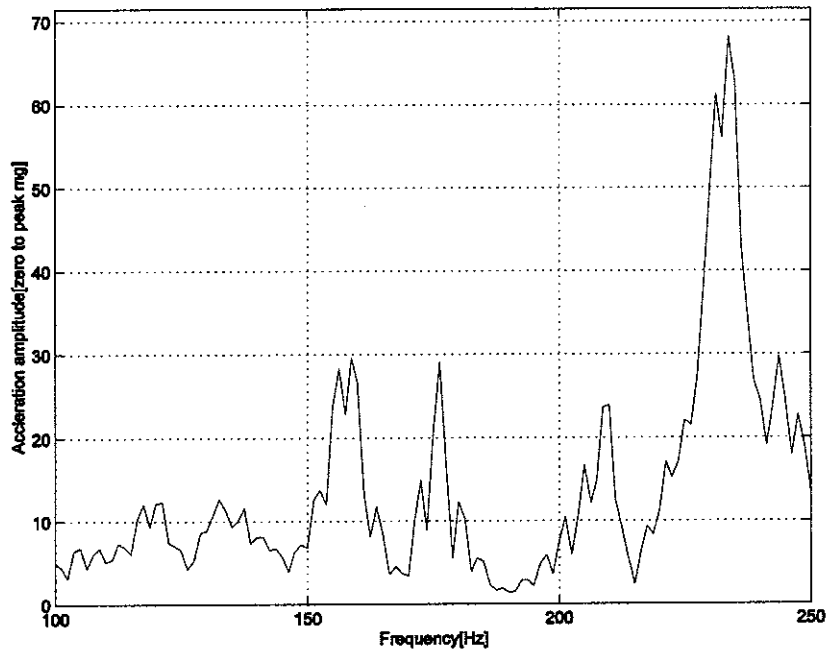

Figure 6. The measured vertical vibration of engine foundation of 9L28/32 generator engine of 5500 TEU container vessel at resilient mount right No.4 position

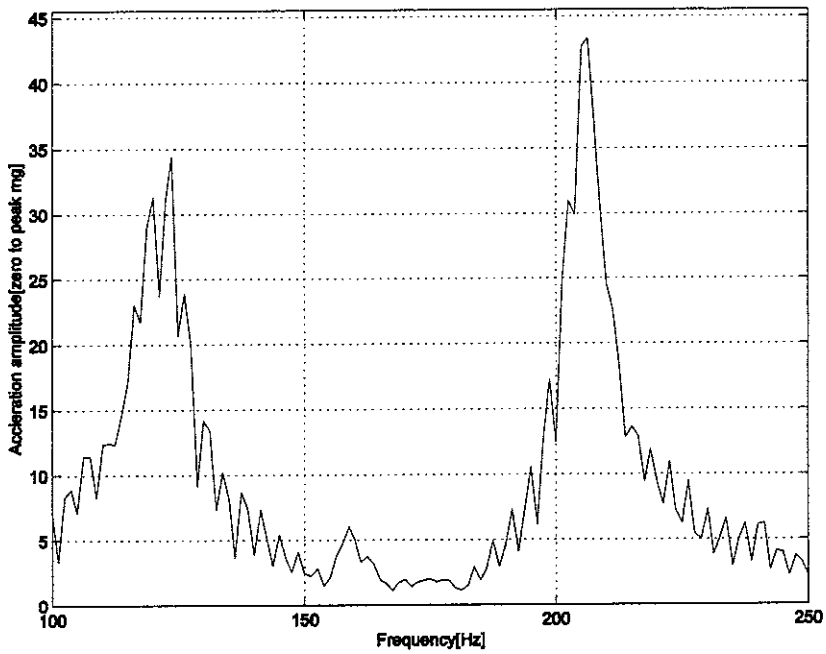

Figure 7. The measured vertical vibration of engine foundation of 9L28/32 generator engine of 5500 TEU container vessel at resilient mount right No.5 position

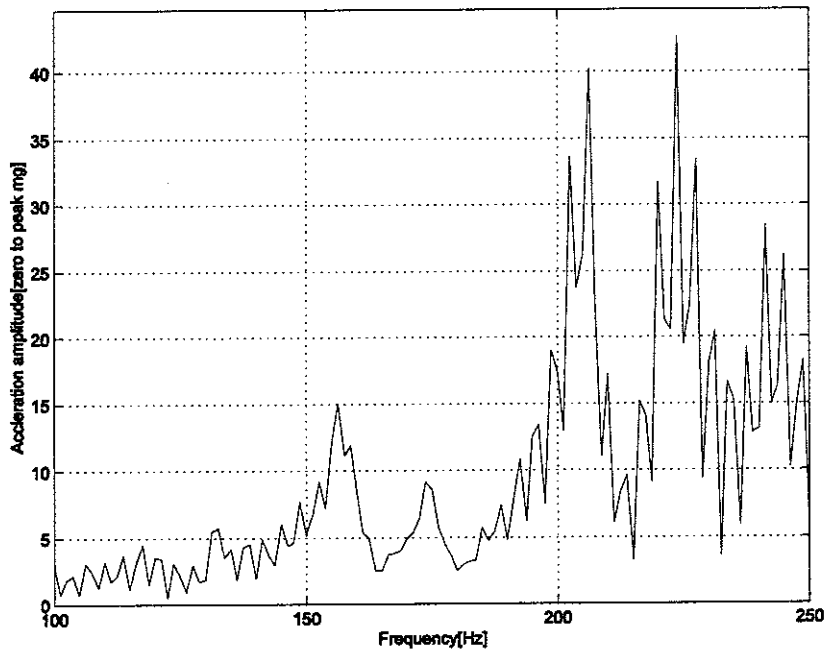

Figure 8. The measured vertical vibration of engine foundation of 9L28/32 generator engine of 5500 TEU container vessel at resilient mount right No.6 position

2.3 Analytical model of a resiliently supported rigid body

Figure 9 shows the general situation for a rigid body supported by resilient mounts. The equations of equilibrium governing the linear dynamic response of a resilient mount system given in matrix form by [15].

$$[M]\cdot\{\ddot{U}\}+[C]\cdot\{\dot{U}\}+[K]\cdot\{U\}=\{R\} \tag{2.3}$$

where $[M]$, $[C]$, $[K]$ are the mass, damping and stiffness matrices, given by $\{U\}$ is the displacement and rotation vector of the centre of gravity,

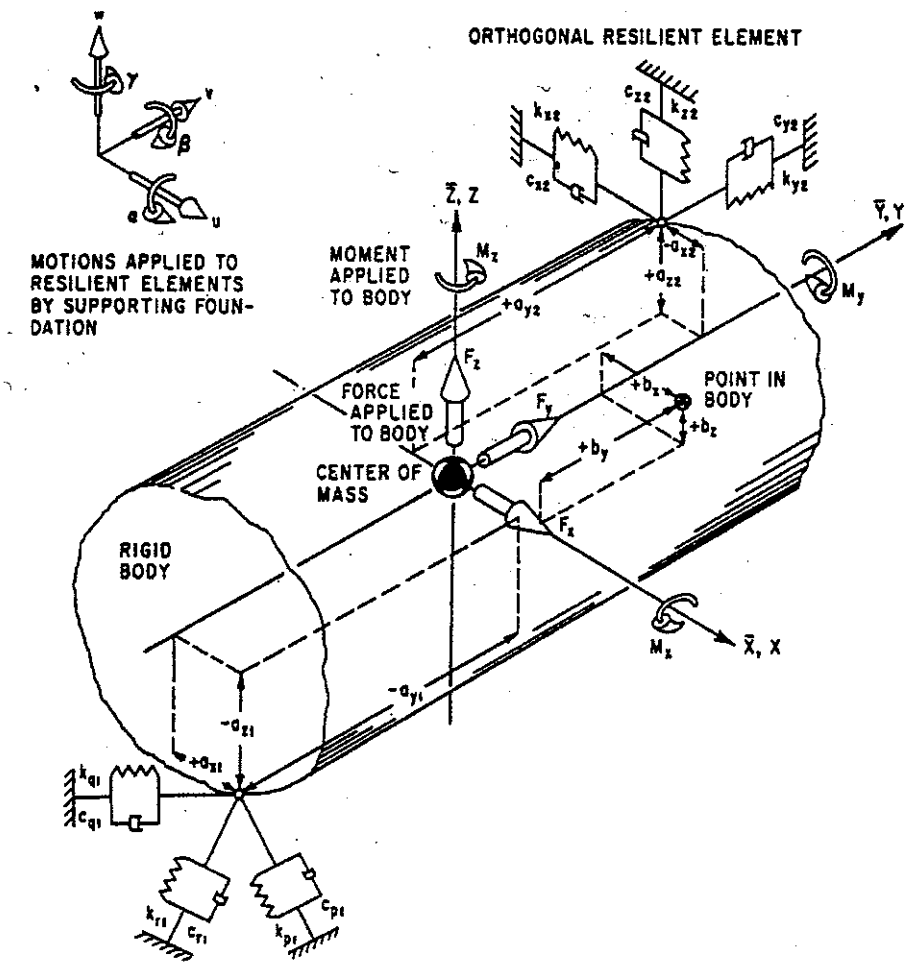

Figure 9. Resilient mount system [15]

$\{R\}$ is the vector of externally applied dynamic load, m is total mass of the diesel engine, generator and common bed, the I's are the 2nd moments of inertia for x, y and z directions, n_r is the total number of resilient mounts and the λ's are cosines of the angles between the principal elastic axes of the resilient supporting elements and the coordinates axes. Here the $[K]$ matrix can be generated by a similar method substituting for C in terms of K.

$$[M]=\begin{bmatrix} m & 0 & 0 & 0 & 0 & 0 \\ 0 & m & 0 & 0 & 0 & 0 \\ 0 & 0 & m & 0 & 0 & 0 \\ 0 & 0 & 0 & I_{xx} & I_{xy} & I_{xz} \\ 0 & 0 & 0 & I_{yx} & I_{yy} & I_{yz} \\ 0 & 0 & 0 & I_{zx} & I_{zy} & I_{zz} \end{bmatrix}, \quad [C]=\begin{bmatrix} C_{11} & C_{12} & C_{13} & C_{14} & C_{15} & C_{16} \\ C_{21} & C_{22} & C_{23} & C_{24} & C_{25} & C_{26} \\ C_{31} & C_{32} & C_{33} & C_{34} & C_{35} & C_{36} \\ C_{41} & C_{42} & C_{43} & C_{44} & C_{45} & C_{46} \\ C_{51} & C_{52} & C_{53} & C_{54} & C_{55} & C_{56} \\ C_{61} & C_{62} & C_{63} & C_{64} & C_{65} & C_{66} \end{bmatrix}, \quad [C]=[C]^T$$

$$[K]=\begin{bmatrix} K_{11} & K_{12} & K_{13} & K_{14} & K_{15} & K_{16} \\ K_{21} & K_{22} & K_{23} & K_{24} & K_{25} & K_{26} \\ K_{31} & K_{32} & K_{33} & K_{34} & K_{35} & K_{36} \\ K_{41} & K_{42} & K_{43} & K_{44} & K_{45} & K_{46} \\ K_{51} & K_{52} & K_{53} & K_{54} & K_{55} & K_{56} \\ K_{61} & K_{62} & K_{63} & K_{64} & K_{65} & K_{66} \end{bmatrix}, \quad [K]=[K]^T, \quad \{U\}=\begin{Bmatrix} x_c \\ y_c \\ z_c \\ \alpha_c \\ \beta_c \\ \gamma_c \end{Bmatrix}, \quad \{R\}=\begin{Bmatrix} F_x \\ F_y \\ F_z \\ M_x \\ M_y \\ M_z \end{Bmatrix}$$

$$C_{11}=\sum_{i=1}^{n_r} C_{xx,i}, \quad C_{12}=\sum_{i=1}^{n_r} C_{xy,i}, \quad C_{13}=\sum_{i=1}^{n_r} C_{xz,i}, \quad C_{14}=\sum_{i=1}^{n_r} (C_{xz,i}\cdot a_{y,i}-C_{xy,i}\cdot a_{z,i}),$$

$$C_{15}=\sum_{i=1}^{n_r} (C_{xx,i}\cdot a_{z,i}-C_{xz,i}\cdot a_{x,i}), \quad C_{16}=\sum_{i=1}^{n_r} (C_{xy,i}\cdot a_{x,i}-C_{xx,i}\cdot a_{y,i}), \quad C_{22}=\sum_{i=1}^{n_r} C_{yy,i}, \quad C_{23}=\sum_{i=1}^{n_r} C_{yz,i},$$

$$C_{24}=\sum_{i=1}^{n_r} (C_{yz,i}\cdot a_{y,i}-C_{yy,i}\cdot a_{z,i}), \quad C_{25}=\sum_{i=1}^{n_r} (C_{xy,i}\cdot a_{z,i}-C_{yz,i}\cdot a_{x,i}),$$

$$C_{26}=\sum_{i=1}^{n_r} (C_{yy,i}\cdot a_{x,i}-C_{xy,i}\cdot a_{y,i}), \quad C_{33}=\sum_{i=1}^{n_r} C_{zz,i}, \quad C_{34}=\sum_{i=1}^{n_r} (C_{zz,i}\cdot a_{y,i}-C_{yz,i}\cdot a_{z,i}),$$

$$C_{35}=\sum_{i=1}^{n_r} (C_{xz,i}\cdot a_{z,i}-C_{zz,i}\cdot a_{x,i}), \quad C_{36}=\sum_{i=1}^{n_r} (C_{yz,i}\cdot a_{x,i}-C_{xz,i}\cdot a_{y,i}),$$

$$C_{44}=\sum_{i=1}^{n_r} (C_{yy,i}\cdot a_{z,i}^2+C_{zz,i}\cdot a_{y,i}^2-2C_{yz,i}\cdot a_{y,i}\cdot a_{z,i}),$$

$$C_{45}=\sum_{i=1}^{n_r} (C_{xz,i}\cdot a_{y,i}\cdot a_{z,i}+C_{yz,i}\cdot a_{x,i}\cdot a_{z,i}-C_{zz,i}\cdot a_{x,i}\cdot a_{y,i}-C_{xy,i}\cdot a_{z,i}^2),$$

$$C_{46}=\sum_{i=1}^{n_r}(C_{xy,i}\cdot a_{y,i}\cdot a_{z,i}+C_{yz,i}\cdot a_{x,i}\cdot a_{z,i}-C_{yy,i}\cdot a_{x,i}\cdot a_{z,i}-C_{xz,i}\cdot a_{y,i}^2),$$

$$C_{55}=\sum_{i=1}^{n_r}(C_{xx,i}\cdot a_{z,i}^2+C_{zz,i}\cdot a_{x,i}^2-2C_{xz,i}\cdot a_{x,i}\cdot a_{z,i}),$$

$$C_{56}=\sum_{i=1}^{n_r}(C_{xy,i}\cdot a_{x,i}\cdot a_{z,i}+C_{xz,i}\cdot a_{x,i}\cdot a_{y,i}-C_{xx,i}\cdot a_{y,i}\cdot a_{z,i}-C_{yz,i}\cdot a_{x,i}^2),$$

$$C_{66}=\sum_{i=1}^{n_r}(C_{xx,i}\cdot a_{y,i}^2+C_{yy,i}\cdot a_{x,i}^2-2C_{xy,i}\cdot a_{x,i}\cdot a_{y,i})$$

$$C_{xx}=C_p\cdot\lambda_{xp}^2+C_q\cdot\lambda_{xq}^2+C_r\cdot\lambda_{xr}^2,\quad C_{yy}=C_p\cdot\lambda_{yp}^2+C_q\cdot\lambda_{yq}^2+C_r\cdot\lambda_{yr}^2,$$

$$C_{zz}=C_p\cdot\lambda_{zp}^2+C_q\cdot\lambda_{zq}^2+C_r\cdot\lambda_{zr}^2,\quad C_{xy}=C_p\cdot\lambda_{xp}\cdot\lambda_{yp}+C_q\cdot\lambda_{xq}\cdot\lambda_{yq}+C_r\cdot\lambda_{xr}\cdot\lambda_{yr},$$

$$C_{xz}=C_p\cdot\lambda_{xp}\cdot\lambda_{zp}+C_q\cdot\lambda_{xq}\cdot\lambda_{zq}+C_r\cdot\lambda_{xr}\cdot\lambda_{zr},\quad C_{yz}=C_p\cdot\lambda_{yp}\cdot\lambda_{zp}+C_q\cdot\lambda_{yq}\cdot\lambda_{zq}+C_r\cdot\lambda_{yr}\cdot\lambda_{zr}$$

$\{U\}$ can be rewritten as

$$\begin{aligned}\{U\}&=A\cdot e^{j(\omega\cdot t+\phi_u)}\ (j=\sqrt{-1}\,)\\&=\{X+j\cdot Y\}\cdot e^{j\omega\cdot t}\ (A=\sqrt{X^2+Y^2}\,,\quad \phi_u=\tan^{-1}\frac{Y}{X})\end{aligned}\tag{2.4}$$

By differentiation of $\{U\}$ and $\{\dot{U}\}$, $\{\dot{U}\}$ and $\{\ddot{U}\}$ can be rewritten as

$$\{\dot{U}\}=\omega\cdot\{-Y+j\cdot X\}\cdot e^{j\omega t}\tag{2.5}$$

$$\{\ddot{U}\}=-\omega^2\cdot\{X+j\cdot Y\}\cdot e^{j\omega t}\tag{2.6}$$

$\{R\}$ can be rewritten as

$$\begin{aligned}\{R\}&=B\cdot e^{j(\omega\cdot t+\phi_r)}\\&=\{V+j\cdot W\}\cdot e^{j\omega\cdot t}\ (B=\sqrt{V^2+W^2}\,,\quad \phi_r=\tan^{-1}\frac{W}{V})\end{aligned}\tag{2.7}$$

Combining equation (2.4)~(2.7), equation (2.3) can be rewritten as

$$([Z_r]\{X\}-[Z_i]\{Y\})+([Z_r]\{Y\}+[Z_i]\{X\})\cdot j=\{V\}+\{W\}\cdot j\tag{2.8}$$

Where $[Z_r]=[K]-\omega^2[M]$ and $[Z_i]=\omega[C]$

In equation (2.8), the real and imaginary parts can be separated as

$$[Z_r]\{X\}-[Z_i]\{Y\}=\{V\} \tag{2.9a}$$

$$[Z_r]\{Y\}+[Z_i]\{X\}=\{W\} \tag{2.9b}$$

In equation (2.9), $\{X\}$, $\{Y\}$ can be rewritten as

$$\{X\}=[E](\{V\}+[D]\{W\}) \tag{2.10a}$$

$$\{Y\}=[E](-[D]\{V\}+\{W\}) \tag{2.10b}$$

Where $[D]=[Z_i][Z_r]^{-1}$ and $[E]=[[Z_r]+[D][Z_r]]^{-1}$

Displacement amplitudes D_x, D_y, D_z of x, y, z directions at arbitrary coordinate $B(b_x, b_y, b_z)$ in figure 9 can be written in terms of the displacement and rotation of the centre of moment as

$$D_x=((x_{cr}+l_z\beta_{cr}-l_y\gamma_{cr})+j(x_{ci}+l_z\beta_{ci}-l_y\gamma_{ci}))e^{j\omega t} \tag{2.11a}$$

$$D_y=((y_{cr}-l_z\alpha_{cr}+l_x\gamma_{cr})+j(y_{ci}-l_z\alpha_{ci}+l_x\gamma_{ci}))e^{j\omega t} \tag{2.11b}$$

$$D_z=((z_{cr}-l_x\beta_{cr}+l_y\alpha_{cr})+j(z_{ci}-l_x\beta_{ci}+l_y\alpha_{ci}))e^{j\omega t} \tag{2.11c}$$

$$x_c=x_{cr}+jx_{ci},\quad y_c=y_{cr}+jy_{ci},\quad z_c=z_{cr}+jz_{ci},$$

$$\alpha_c=\alpha_{cr}+j\alpha_{ci},\quad \beta_c=\beta_{cr}+j\beta_{ci},\quad \gamma_c=\gamma_{cr}+j\gamma_{ci},$$

$$l_x=b_x-g_x,\quad l_y=b_y-g_y,\quad l_z=b_z-g_z$$

The $\frac{j}{2}^{\text{th}}$ (j=1, 2, 3...24) order dynamic forces $S_{x,i,\frac{j}{2}}, S_{y,i,\frac{j}{2}}, S_{z,i,\frac{j}{2}}$ of x, y, z directions at arbitrary resilient mount i can be written as

$$S_{x,i,\frac{j}{2}} = K_{xx,i} \cdot D_{x,i,\frac{j}{2}} + K_{xy,i} \cdot D_{y,i,\frac{j}{2}} + K_{xz,i} \cdot D_{z,i,\frac{j}{2}} \quad (2.12a)$$

$$S_{y,i,\frac{j}{2}} = K_{xy,i} \cdot D_{x,i,\frac{j}{2}} + K_{yy,i} \cdot D_{y,i,\frac{j}{2}} + K_{yz,i} \cdot D_{z,i,\frac{j}{2}} \quad (2.12b)$$

$$S_{z,i,\frac{j}{2}} = K_{xz,i} \cdot D_{x,i,\frac{j}{2}} + K_{yz,i} \cdot D_{y,i,\frac{j}{2}} + K_{zz,i} \cdot D_{z,i,\frac{j}{2}} \quad (2.12c)$$

where $D_{x,i,\frac{j}{2}}, D_{y,i,\frac{j}{2}}, D_{z,i,\frac{j}{2}}$ are the $\frac{j}{2}^{\text{th}}$ order displacement amplitudes of x, y, z directions at arbitrary resilient mount i, $K_{xx,i}, K_{yy,i}, K_{zz,i}$ are stiffness of x, y, z directions, $K_{xy,i}, K_{yz,i}, K_{xz,i}$ are stiffness of xy, yz, xz planes at arbitrary resilient mount i. Synthesized dynamic forces from 0.5^{th} to 12^{th} $S_{sx,i}$, $S_{sy,i}$, $S_{sz,i}$ in x, y and z directions of resilient mount i can be written as

$$S_{sx,i} = \frac{1}{2}(|S_{x\max,i}| + |S_{x\min,i}|) \quad (2.13a)$$

$$S_{sy,i} = \frac{1}{2}(|S_{y\max,i}| + |S_{y\min,i}|) \quad (2.13b)$$

$$S_{sz,i} = \frac{1}{2}(|S_{z\max,i}| + |S_{z\min,i}|) \quad (2.13c)$$

where $S_{x\max,i}, S_{y\max,i}, S_{z\max,i}$ are the maximum valves and $S_{x\min x,i}, S_{y\min,i}, S_{z\min,i}$ are the minimum valves in x, y, z directions at arbitrary resilient mount i during two revolutions of crank shaft(720 degrees).

Even through the phase angles of maximum values in x, y and z direction is are equal, in the worst case, the synthesized dynamic force $S_{s,i}$ of three directions of resilient mount i can be

written as

$$S_{s,i} = \sqrt{S_{sx,i}^2 + S_{sy,i}^2 + S_{sz,i}^2} \tag{2.14}$$

2.4 Exciting force and moment in diesel engine

Figure 10 shows the force transmission mechanism in one cylinder of an internal combustion engine. The force F can be split into a force in the direction of be connecting rod F_C, and a horizontal force F_S. Here

$$F_C = \frac{F}{\cos\delta} \tag{2.15}$$

where F is $F_P + F_{REP}$, and F_P is the force generated by combustion pressure within the cylinder, and F_{REP} is the inertia force generated by the reciprocating masses of the piston and part of the connecting rod. Furthermore, the tangential component of the force F_C is

$$F_T = F_C \cdot \sin(\theta + \delta) \tag{2.16}$$

$$\text{and } H_{TNG} = \frac{F_T}{A_C} \tag{2.17}$$

where H_{TNG} is the tangential harmonic coefficient (N/mm^2) for torsional vibration calculations and is provided by the engine manufacturer or it can be obtained by the measurements of the combustion pressure within the cylinder. A_C is the section area of the cylinder $(\frac{\pi}{4}D^2)$ and D is the cylinder bore (mm). Again, referring to figure 10

$$F_N = F_C \cdot \cos(\theta + \delta) \tag{2.18}$$

$$\text{and } H_{RDL} = \frac{F_N}{A_C} \tag{2.19}$$

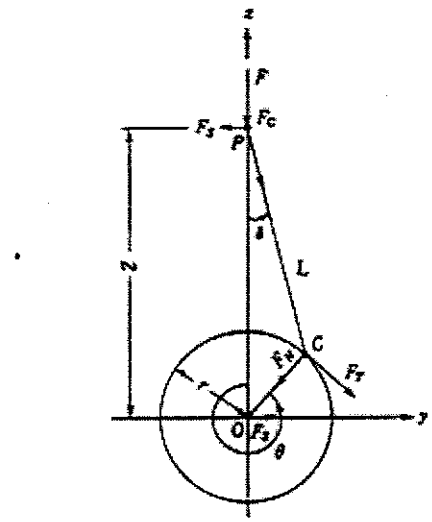

Figure 10. Guide force of crankshaft and connection rod
in one cylinder of internal combustion engine

where H_{RDL} is the radial harmonic coefficient (N/mm^2) for axial vibration calculations and it is provided by the engine manufacturer or it can be obtained by the measurement of the combustion pressure within the cylinder. The guide force and H-type guide force moment in one cylinder of the internal combustion engine shown in figure 11, F_S and M_G are defined by

$$\begin{aligned} F_S &= F \cdot \tan\delta \\ &= F_C \sin\delta \\ &= F_T \frac{\sin\delta}{\sin(\theta+\delta)} \end{aligned} \tag{2.20}$$

$$\begin{aligned} M_G &= F_S \cdot Z \\ &= F_S \cdot (L\cdot\cos\delta + r\cdot\cos\theta) \\ &\quad (L\cdot\sin\delta = r\cdot\sin\theta) \\ &= F_S \cdot r\frac{(\sin\theta\cdot\cos\delta + \cos\theta\cdot\sin\delta)}{\sin\delta} \\ &= F_T \cdot r \end{aligned} \tag{2.21}$$

For the total H-type guide force moment of k^{th} order with n cylinders, equation (2.21) can be written as

$$M_{H,k} = \sum_{i=1}^{n} H_{TNG,k} \cdot A_C \cdot r \cdot \sin\{k(\theta + \alpha_{e,i}) + \beta_{e,k}\} \qquad (2.22)$$

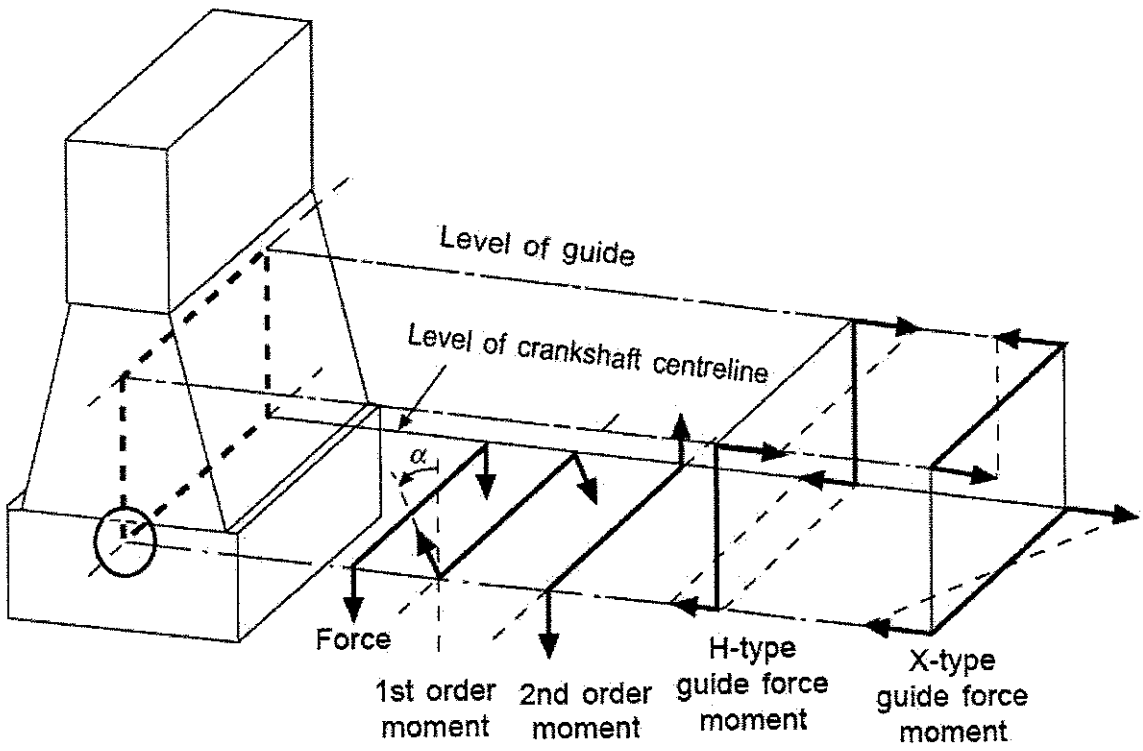

Figure 11. Force and moment of multi-cylinder diesel engine

where k is the harmonic order, n is the numbers of cylinder, $r(m)$ is half the stroke, $\alpha_{e,i}$ is the initial crank angle at cylinder i, and $H_{TNG,k}$ is the k^{th} order tangential harmonic coefficient and $\beta_{e,k}$ is the phase angle of the k^{th} order tangential harmonic coefficient.

In even crank angle four stroke engines k is $\frac{n}{2}, n, \frac{3n}{2}, 2n, \ldots\ldots$ or in even crank angle of two stroke engines k is $n, 2n, 3n, \ldots\ldots$, and equation (2.22) can be rewritten as

$$M_{H,k}(M_x \text{ in } \alpha \text{ direction in figure } 9) = n \cdot H_{TNG,k} \cdot A_C \cdot r \cdot \sin(k \cdot \theta + \beta_{e,k}) \quad (2.23)$$

Combining equations (2.17) and (2.20), the total X-type guide force moment of k^{th} order in figure 11 and 12 is determined by [16]

$$M_{X,k} = \sum_{i=1}^{n} F_S \cdot \sin\{k(\theta + \alpha_{e,i}) + \beta_{e,k}\} \cdot l_i \quad (2.24)$$

$$\begin{aligned} F_S &= F_T \frac{\sin\delta}{\sin(\theta+\delta)} \\ &= F_T \frac{\lambda_e \cdot \sin\theta}{\{\sin\theta \cdot (1-\lambda_e^2 \cdot \sin\theta^2) + \cos\theta \cdot \lambda_e \cdot \sin\theta\}} \\ &= \lambda_e \cdot F_T \frac{1}{(1-\lambda_e^2 \cdot \sin\theta^2 + \lambda_e \cdot \cos\theta)} \\ &= \lambda_e \cdot F_T \cdot A_f \end{aligned} \quad (2.25)$$

where L is the length of the connecting rod, λ_e is $\frac{r}{L}$, $A_f = \frac{1}{(1-\lambda_e^2 \cdot \sin\theta^2 + \lambda_e \cdot \cos\theta)}$) and l_i is the longitudinal distance of cylinder i from the engine centre in the x direction.

Using equation (2.25), equation (2.24) can be rewritten as

$$M_{X,k}(M_z \text{ in } \gamma \text{ direction in figure } 9) = \lambda_e \cdot H_{TNG,k} \cdot A_f \cdot \sum_{i=1}^{n} l_i \cdot \sin\{k(\theta + \alpha_{e,i}) + \beta_{e,k}\} \quad (2.26)$$

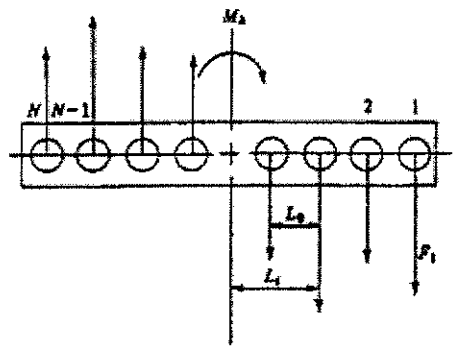

Figure 12. X-type guide force moment for internal combustion engine

Figure 13 shows the factor A_f when λ_e is 0.25 (the value of the test model engine in this report), and it is convenient to use the average value for the X-type guide force moment calculation.

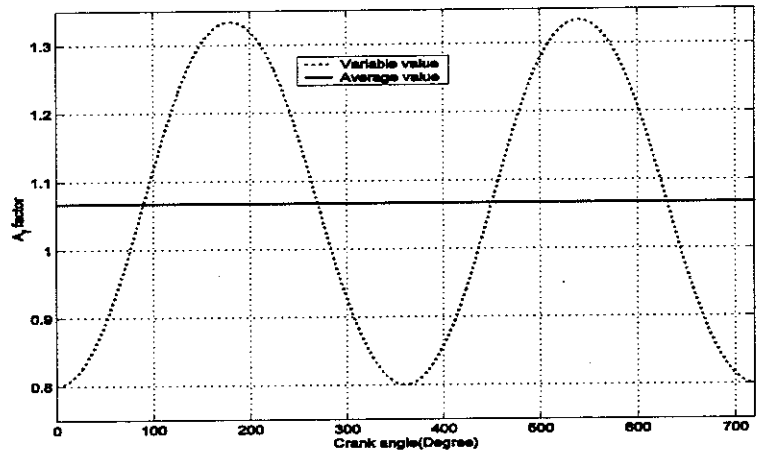

Figure 13. A_f factor of 9L28/32 engine in X-moment calculation

The vertical and horizontal unbalance forces in one cylinder of the internal combustion engine, F_H and F_V are defined by

$$F_H = m_C \cdot r \cdot \omega^2 \cdot \sin\theta \tag{2.27}$$

$$F_V = m_C \cdot r \cdot \omega^2 \cdot \cos\theta + m_{REP} \cdot r \cdot \omega^2 \cdot (\cos\theta + \lambda_e \cdot \cos 2\theta) \tag{2.28}$$

where m_C is the unbalanced mass of the crank throw and connecting rod, m_{REP} is the reciprocating mass of the piston and connecting rod and ω is the angular velocity of the crank shaft. Separating forces of 1st and 2nd order components, equation (2.27) and (2.28) can be rewritten as

$$F_{H1} = m_C \cdot r \cdot \omega^2 \cdot \sin\theta \tag{2.29}$$

$$F_{V1} = (m_C + m_{REP}) \cdot r \cdot \omega^2 \cdot \cos\theta \tag{2.30}$$

$$F_{V2} = m_{REP} \cdot r \cdot \omega^2 \cdot \lambda_e \cdot \cos 2\theta \tag{2.31}$$

The 1st horizontal, and 1st and 2nd vertical forces in the internal combustion engine with n cylinders, F_{SH1}, F_{SV1} and F_{SV2} are defined by

$$F_{SH1}(\,F_y \ in \ y \ direction \ in \ figure \ 9\,) = m_C \cdot r \cdot \omega^2 \cdot \sum_{i=1}^{n} \sin(\theta + \alpha_{e,i}) \tag{2.32}$$

$$F_{SV1}(\,F_y \ in \ y \ direction \ in \ figure \ 9) = (m_C + m_{REP}) \cdot r \cdot \omega^2 \cdot \sum_{i=1}^{n} \cos(\theta + \alpha_{e,i}) \tag{2.33}$$

$$F_{SV2}(\,F_z \ in \ z \ direction \ in \ figure \ 9\,) = m_{REP} \cdot r \cdot \omega^2 \cdot \lambda_e \cdot \sum_{i=1}^{n} \cos 2(\theta + \alpha_{e,i}) \tag{2.34}$$

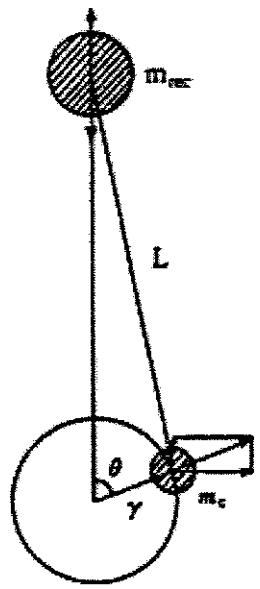

Figure 14. External force for a cylinder engine

The 1st horizontal, 1st and 2nd vertical unbalance moment in the internal combustion engine with n cylinders, M_{SH1}, and M_{SV1} and M_{SV2} are defined by

$$M_{SH1}(M_z \text{ in } \gamma \text{ direction in figure 9}) = m_C \cdot r \cdot \omega^2 \cdot \sum_{i=1}^{n} l_i \cdot \sin(\theta + \alpha_{e,i}) \quad (2.35)$$

$$M_{SV1}(M_y \text{ in } \beta \text{ direction in figure 9}) = (m_C + m_{REP}) \cdot r \cdot \omega^2 \cdot \sum_{i=1}^{n} l_i \cdot \cos(\theta + \alpha_{e,i}) \quad (2.36)$$

$$M_{SV2}(M_y \text{ of } \beta \text{ direction in figure 9}) = m_{REP} \cdot r \cdot \omega^2 \cdot \lambda_e \cdot \sum_{i=1}^{n} l_i \cdot \cos 2(\theta + \alpha_{e,i}) \quad (2.37)$$

2.5 Design evaluation for mechanical vibration of marine diesel engine generator

The measuring point and vibration level recommended by ISO [17] is shown in Figure 15 and 16 respectively. This guidance is not a quantitative analysis method.

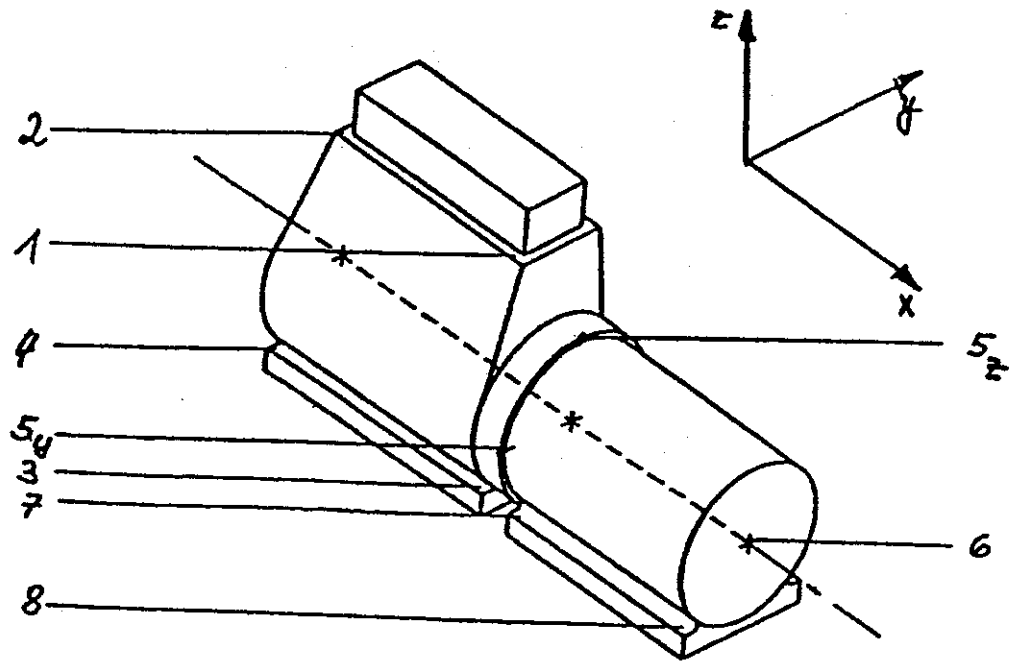

Figure 15. Vibration measuring positions recommended by ISO 8528-9

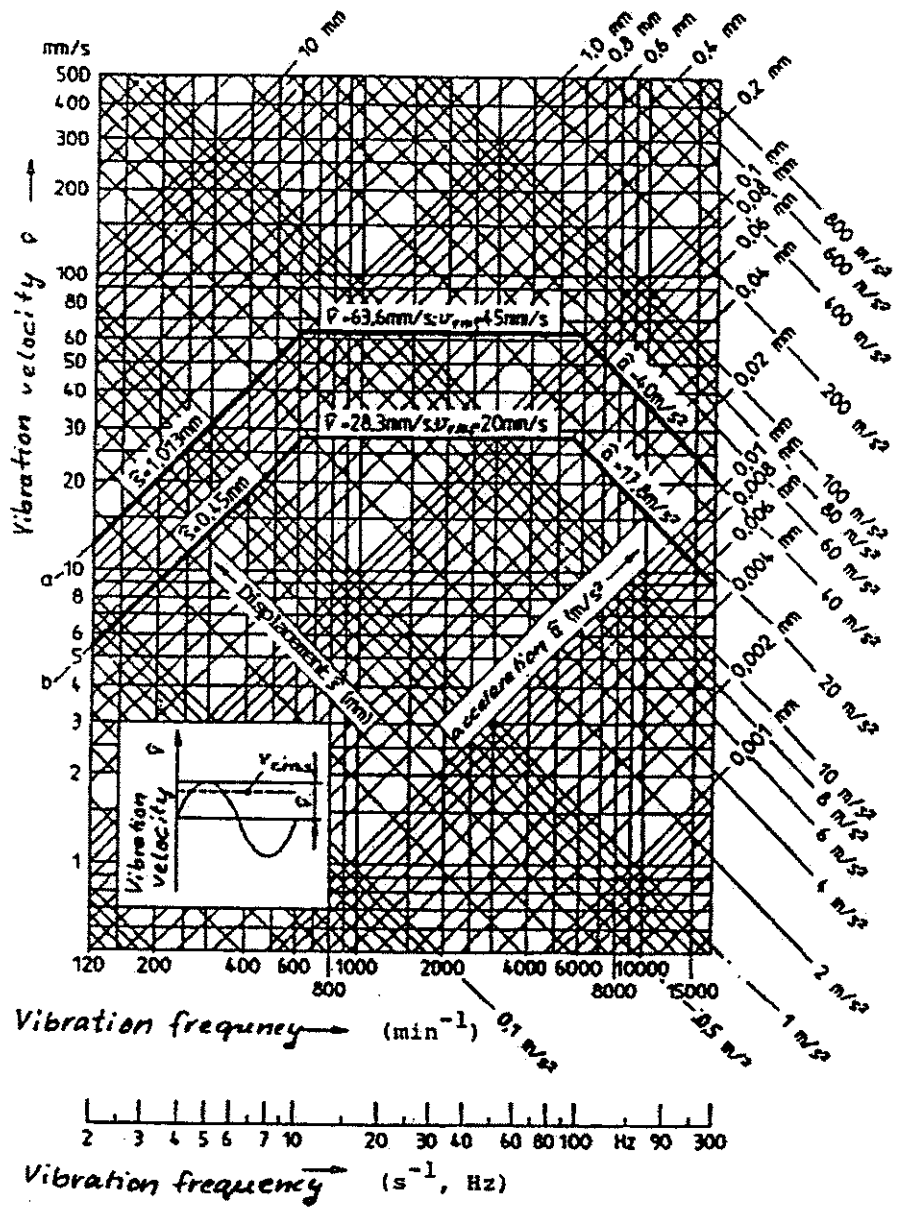

Figure 16. Guide line of mechanical vibration recommended by ISO 8528-9

In view of the secondary vibration of the structure in the hull deck and the lifetime of resilient mounts, it is important to evaluate the dynamic force and elastic potential energy stored from the resilient mounts. Thus a method is proposed as follows.

The ratio of the dynamic force to the total weight using equation (2.14) in engine operation mode p (see table 4) can be written as

$$DFR_{t,p} = \frac{\sum_{i=1}^{n_r} S_{s,i}}{mg} \tag{2.38}$$

The weighted dynamic force ratio can be rewritten as

$$DFR_w = \frac{\sum_{p=1}^{n_p} DFR_{t,p} \cdot wt_p}{\sum_{p=1}^{n_p} wt_p} \tag{2.39}$$

where n_p is total number of the engine operation modes and wt_p is the weighting factor in engine operation mode p.

In this report we propose that the vibration activity of the engine and supports is measured by a single number that is related to the elastic potential energy stored in the resilient mounts. This number is referenced to as the elastic potential energy index(or activity index) and is defined by

$$EPE_{t,p} = 2\pi \sum_{i=1}^{n_r} \left(\sum_{j=1}^{24} \left(\frac{j}{2} \cdot \frac{rpm}{60} \right)^2 \cdot \left(\left| S_{x,i,\frac{j}{2}} \right| \cdot \left| D_{x,i,\frac{j}{2}} \right| + \left| S_{y,i,\frac{j}{2}} \right| \cdot \left| D_{y,i,\frac{j}{2}} \right| + \left| S_{z,i,\frac{j}{2}} \right| \cdot \left| D_{z,i,\frac{j}{2}} \right| \right) \right) \tag{2.40}$$

where rpm is engine speed(revolution per min) and $\frac{j}{2}$ is the order for vibration. This index is related to the maximum energy that might be stored the mounts. The actual energy is also related to the phase of the response harmonics of $D_{x,i,\frac{j}{2}}$, $D_{y,i,\frac{j}{2}}$, $D_{z,i,\frac{j}{2}}$ the index represents a "worst case" behaviour. If K_{xy}, K_{xz}, K_{yz} are zero in equation (2.12), equation (2.40) can be rewritten as

$$EPE_{t,p} = \frac{1}{4\pi}\sum_{i=1}^{n_r}\left(\sum_{j=1}^{24}\left(K_{xx,i}\cdot\left|v_{x,i,\frac{j}{2}rms}\right|^2 + K_{yy,i}\cdot\left|v_{y,i,\frac{j}{2}rms}\right|^2 + K_{zz,i}\cdot\left|v_{z,i,\frac{j}{2}rms}\right|^2\right)\right) \quad (2.41)$$

where $v_{x,i,\frac{j}{2}rms}$, $v_{y,i,\frac{j}{2}rms}$, $v_{z,i,\frac{j}{2}rms}$ are the velocity amplitudes(root mean square) for x, y and z directions in resilient mount i. The elastic potential energy index as a sum of cross sectional area in the resilient mounts in engine operation mode p (see table 4) can be written as

$$EPE_{r,p} = \frac{EPE_{t,p}}{A_r} \quad (2.42)$$

where A_r is the sum of cross sectional area in the resilient mounts. The elastic potential energy index to weighting factor can be written as

$$EPE_w = \frac{\sum_{p=1}^{n_p} EPE_{r,p}\cdot wt_p}{\sum_{p=1}^{n_p} wt_p} \quad (2.43)$$

The classification method of four stroke diesel engine generator for marine vessels is shown in Table 3. The weighting factor for engine operation mode based on the authors' experience is shown in Table 4 and these may be changed according to the use, purpose and frequency of the ship. It is desirable that the dynamic force ratio at the peak resonance point at medium engine speed with normal firing as shown in table 4 does not exceed 20 % based on authors' experience. The elastic potential energy index of the resilient mount should be discussed and decided with the manufacturer. For different engines the weighted average value of dynamic force ratio and elastic potential energy index for optimum design can be compared and should be designed to be as small as possible.

Table 3 Classification of four stroke marine diesel engines based on maximum continuous rating

Classification	Engine speed range(rpm)
Low speed(A)	Below 599
Medium speed(B)	600~999
High speed(C)	Above 1,000

Table 4 Weighting factor for mechanical vibration evaluation

No.	Cylinder firing condition	Operation range for engine speed	Weighting factor
1	Normal firing and generator full load with 10 % uneven firing(P1)	from 90 to 110 % of synchronized speed	1.0
2	One cylinder misfiring and generator 70% load(P2)	from 90 to 110 % of synchronized speed	0.25
3	Normal firing and generator no load with 25 % uneven firing(P3)	from minimum revolution to 110 % of synchronized speed	0.5
4	One cylinder misfiring and generator no load (P4)	from minimum revolution to 110 % of synchronized speed	0.25

3. THEORETICAL VIBRATION ANALYSIS FOR TEST MODEL

3.1 Free vibration

The marine diesel engine generator of a 5,500TEU container vessel was selected as a vibration analysis and test model. The specification of the engine, bedplate and generator are shown in Table 5. The moments of inertia are I_{xx} 20,697 kg.m^2, I_{yy} 250,080 kg.m^2, I_{zz} 240,010 kg.m^2 and $I_{xy} = I_{xz} = I_{yz} = 0$. The main exciting moments at full load and synchronized speed are 1st order vertical(M_{V1})=24.3, 1st order transverse(M_{H1})=12.1, 2nd order vertical(M_{V2})=11.3, 4.5th order H-type guide force moment=22.6 and 9th order H-type guide force moment= 4.3 kN-m. The resilient mount arrangement is shown in figure 17. The natural frequencies and relative vibration modes are shown in table 6. The right and left resilient mount rows from the centre line are designed and installed in a symmetrical arrangement. However the turbocharger bellows is connected with one point of non-symmetry. Even though the vibration of the y direction (No.1) is mainly coupled with α direction and other directions have a very small couple effect by the stiffness of turbocharger bellows. Otherwise the vibration mode of β (No.2), x (No. 5) and α (No. 6) directions is coupled with the x, β and y direction each other. And if the effect of the turbocharger bellows is neglected, the vibration mode of z (No.2) and γ (No.4) are not coupled in any direction.

Table 5 Specification of test engine model

Diesel engine	Type	9L28/32
	Cylinder bore	280 mm
	Stroke	320 mm
	Power	2,540 hp
	Mean indicated pressure	21.3 bar(full load) 2.0 bar(no load)
	Reciprocating mass	87.8 kg/cyl.
	Firing order	1-5-9-3-6-8-2-4-7
	Conn. ratio(r/l)	0.25
	No. of cylinder	9
	Idling speed	180 rpm
	Weight	34,000 kg(dry)
Common bed	Breadth	1,700 mm
	Height	685 mm
	Total length	7,360 mm
	Weight	2,150 kg
Generator	Synchronized speed	720 rpm
	M.O.I (rotor)	328.95 kg·m^2
	Weight	2,425 kg
	No. of poles	10

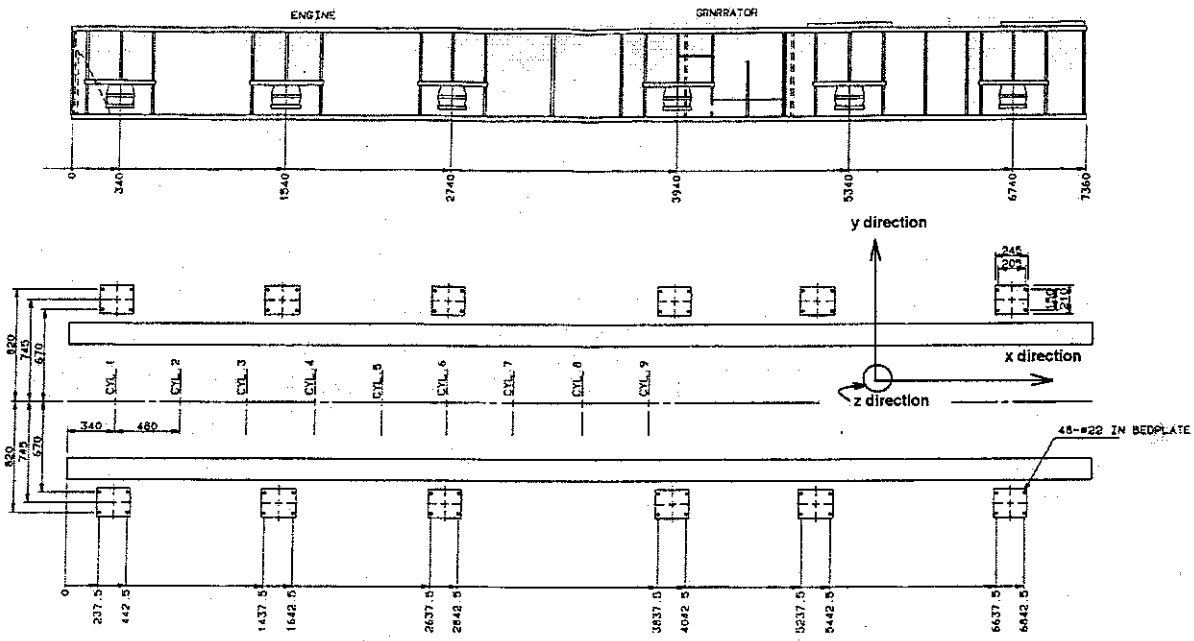

Figure 17. The resilient mount arrangement for 9L28/32 engine generator(Unit: mm)

Table 6. Natural frequencies and vibration modes for marine diesel engine generator

No.	Natural frequencies (cycle/min)	Relative amplitude(mm and mrad)					
		x	y	z	α	β	γ
1	245.02 (y)	-0.00228	1.00000	-0.01600	-0.79071	-0.00178	0.00728
2	329.36 (β)	1.00000	0.00640	-0.00795	-0.00348	0.53925	-0.00214
3	404.14 (z)	0.00451	0.00148	1.00000	-0.00038	0.00115	0.00000
4	461.54 (γ)	0.00350	-0.03487	0.00000	0.01035	0.00272	1.00000
5	526.20 (x)	1.00000	-0.00118	-0.00238	-0.00039	-0.33517	0.00028
6	862.76 (α)	0.00010	0.36200	-0.0036	1.00000	-0.00027	0.00149

3.2 Forced vibration

The forced vibration calculation was performed for the four cases shown in table 4. The major exciting sources in the test model engine are 1st, 2nd order unbalance moments and 4.5th order H-type guide force moment. The velocity amplitudes of major points with all of the cylinders firing normally and for a generator full load condition at synchronized speed are shown in table 7. The velocity amplitudes compared to the ISO 8528-9 guide line are small. Detailed calculation results of resilient mounts right No.1, No. 4, No.5, No.6 and engine top-fore, top-aft for above 4 cases are shown in appendix A figures A1~A24. The total dynamic force(DFR_w) for the four cases of table 4 are shown in table 8. The total value is 7.5% and evenly affected by all modes of engine operation. Detailed calculation results for dynamic force are shown in appendix A figures A25~A32. The total elastic potential energy index for the four cases of table 4 is shown in table 9. The total value is 13.56 kW/m^2. It is mainly effected by the 4.5th resonance due to the H-type guide force moment in operation mode P3 and P4. Detailed calculation results for the dynamic force are shown in appendix A figures A33~A40.

Table 7. The velocity amplitudes at full load and synchronized speed(unit : mm/s)

Position	Direction	1st order	1.5th order	2nd order	4.5th order
Center of gravity	x	1.3	0.0	0.0	0.0
	y	0.7	0.2	0.0	0.1
	z	0.0	0.0	0.0	0.0
Resilient mount right No. 1	x	4.0	0.0	0.3	0.0
	y	4.4	1.0	0.3	3.2
	z	6.1	0.7	0.9	2.5
Resilient mount right No. 4	x	4.0	0.0	0.3	0.0
	y	1.5	1.0	0.3	3.2
	z	1.5	0.7	0.3	2.5
Turbocharger bellows	x	4.9	0.0	0.8	0.0
	y	4.1	2.1	0.8	8.3
	z	8.8	0.9	1.5	3.6
Engine top-fore (exhaust side)	x	1.0	0.0	0.2	0.0
	y	3.7	0.5	0.2	2.6
	z	7.3	0.6	1.2	2.2
Engine top-aft (exhaust side)	x	1.0	0.0	0.2	0.0
	y	1.4	0.5	0.2	2.6
	z	2.3	0.6	0.4	2.2

Table 8. Total dynamic force(ratio to weight)

Operation mode (In table 4)	Dynamic force($DFR_{t,p}$)	Weighting factor(wt_p)	$\frac{DFR_{t,p} \cdot wt_p}{\sum_{p=1}^{n_p} wt_p} \times 100(\%)$
P1	0.042	1.00	2.1
P2	0.135	0.25	1.7
P3	0.066	0.5	1.7
P4	0.161	0.25	2.0
Summation(DFR_w)	-	2	7.5

Table 9. Total elastic potential energy index(kW/m^2)

Operation mode (In table 4)	Elastic potential energy index($EPE_{r,p}$)	Weighting factor(wt_p)	$\frac{EPE_{r,p} \cdot wt_p}{\sum_{p=1}^{n_p} wt_p}$
P1	3.53	1.00	1.77
P2	29.85	0.25	3.73
P3	15.40	0.5	3.85
P4	33.71	0.25	4.21
Summation(EPE_w)	-	-	13.56

4. Validation of analytical models

4.1 Outline for vibration test

A schematic diagram and pictures of the mechanical vibration and structure-borne noise measurement set up are shown in figures 18~20. A total of six accelerometers and two signal conditioners were installed at x, y and z direction of resilient mount number 1 and 4. An optical sensing tachometer was located at the free end of the generator shaft. The speed of the generator engine on board ship could not be controlled by the governor. To investigate the resonances of the diesel engine generator with resilient rubber mounts the engine was started and stopped repeatedly. Then all of the signals via A/D converter with sampling rate of 2048 samples/second were stored in a laptop computer. The structure-borne noise and mechanical vibration at synchronized generator speed of 720 rpm were measured by a portable 2 channel FFT analyzer type DI 2200. Signal analysis of the stored vibration signals was performed by two methods. Firstly, spectral analysis was performed on the stored digital data using a 16384-point FFT, a Hanning window with 75% overlap and power spectrum averaging. Secondly, order analysis for engine speed was performed on the stored digital data using a Discrete Fourier Transform by two revolution intervals.

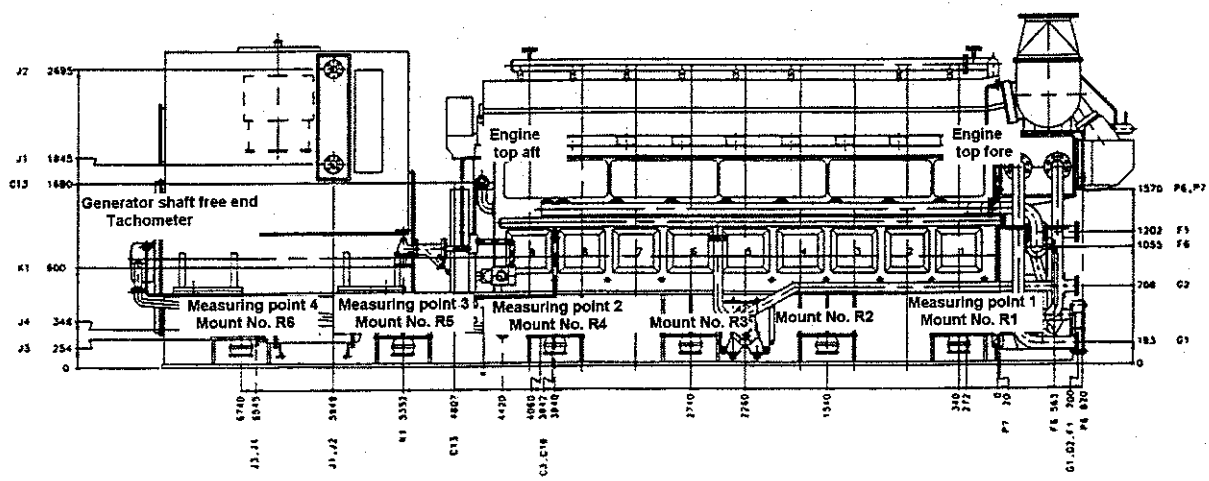

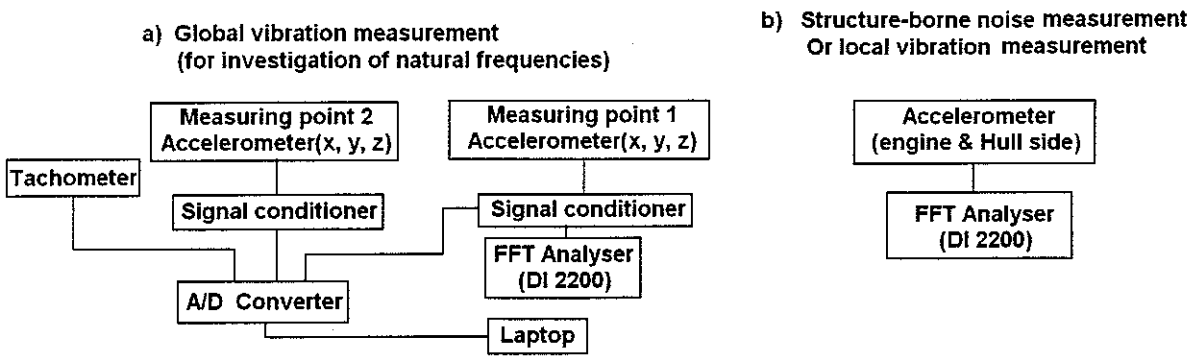

Figure 18. Schematic diagrams for mechanical vibration and structure-borne noise measurement.

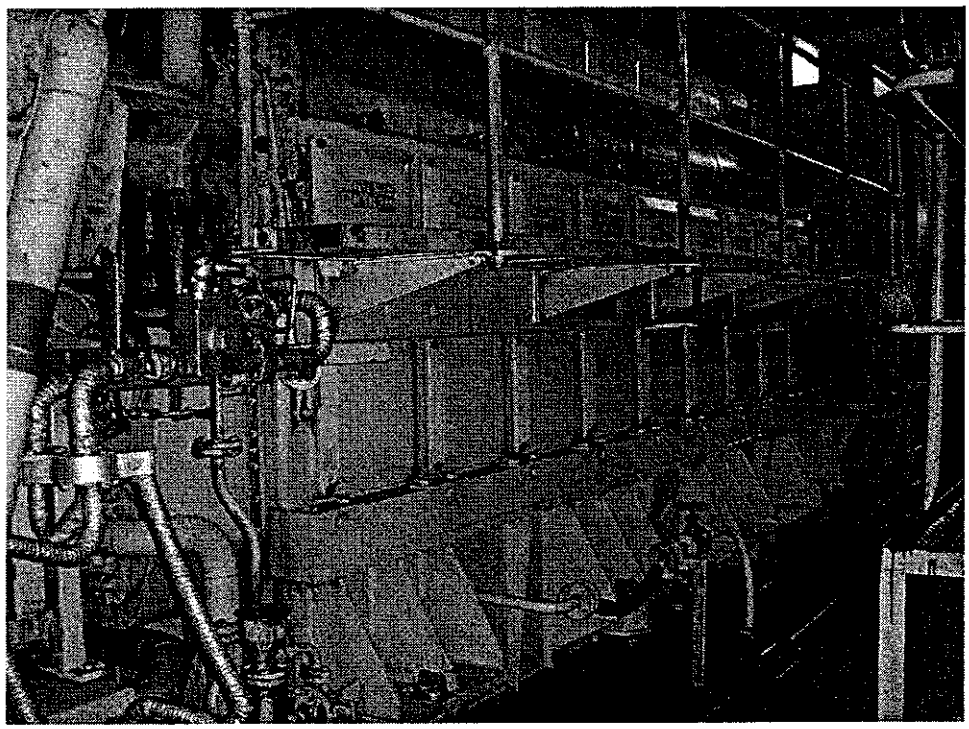

Figure 19. Overview for test(9L28/32) engine with resilient mounts

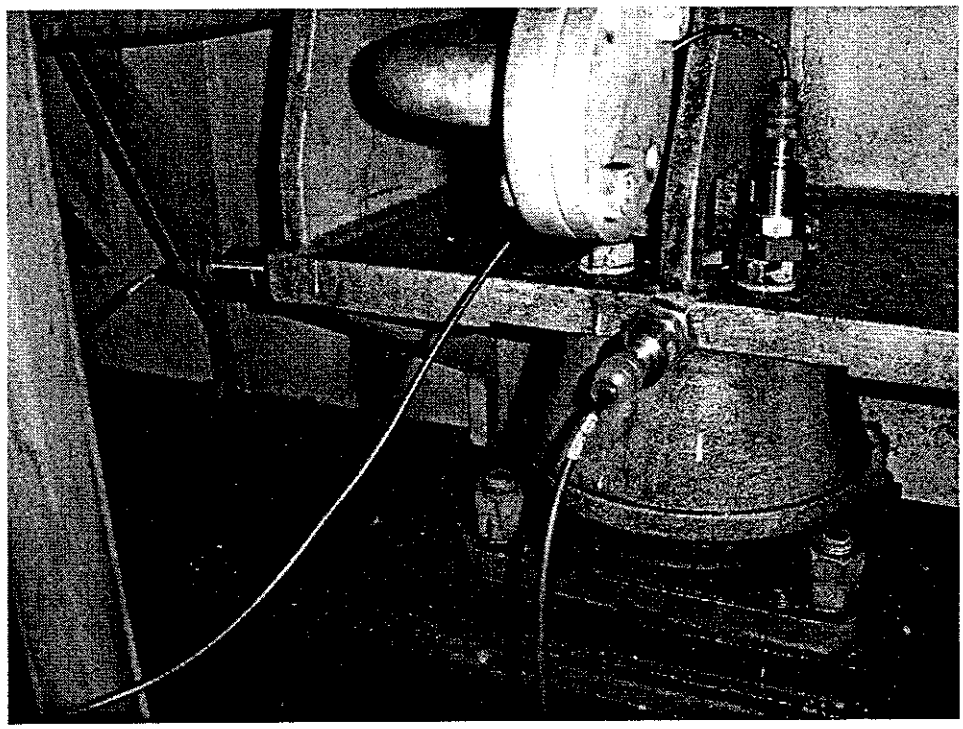

Figure 20. Accelerometers attached at resilient mounts right No. 4

4.2 Natural frequencies

Figure 21 shows engine speed during the diesel generator start-up with fuel injection. Natural frequencies from measured data could not be confirmed in this short time. Figure 22~23 show the 1^{st} order vibration of the resilient mounts in horizontal-transverse (y). Figure 24~25 show the 4.5^{th} order vibration of resilient mounts in horizontal-transverse. The large vibration near 600 rpm in figure 25 may be due to torsional vibration. Figure 26 shows engine speed during the run-down of the diesel generator with the fuel cut-off and the run-down time was long compared to that of the run-up. The natural frequencies of body vibration for the diesel engine generator can be determined from these data. Figure 27 show the 1^{st} order velocity amplitudes in horizontal-transverse direction. Figure 28~29 show the 4.5^{th} order velocity amplitudes in the horizontal-transverse direction. The vibration peaks (H-type mode) of two resilient mount points near 230 rpm have the same amplitudes and two peaks(flexible mode)[18] near 340 rpm have different

amplitudes. The H-type mode and the flexible mode of vibration can be distinguished from these results. Figures 30~35 show the contour results by FFT analysis. Table 10 shows comparison table of calculation and measurement result and these correspond well with the calculation of the engine's elastic foundation.

Table 10. Comparison of calculation and measurement of natural frequencies for mechanical vibration of diesel engine generator.

Node	Vibration direction	Natural frequencies (Cycle per min)		
		Calculation (rigid)	Calculation (engine's elastic foundation)	Measured
1st	y	250.25	245.02	255.0(4.25Hz)
2nd	β (y-rotation)	336.93	329.36	329.4(5.49 Hz)
3rd	z	416.00	404.14	404.6(6.70 Hz)
4th	γ (z-rotation)	461.54	461.54	450.0(7.5 Hz)
5th	x	529.33	526.20	495.0(8.25 Hz)
6th	α (x-rotation)	868.08	862.76	997.345(14.08 Hz)
Flexible mode of common bed	Structure torsion		-	1544.58(25.74 Hz)

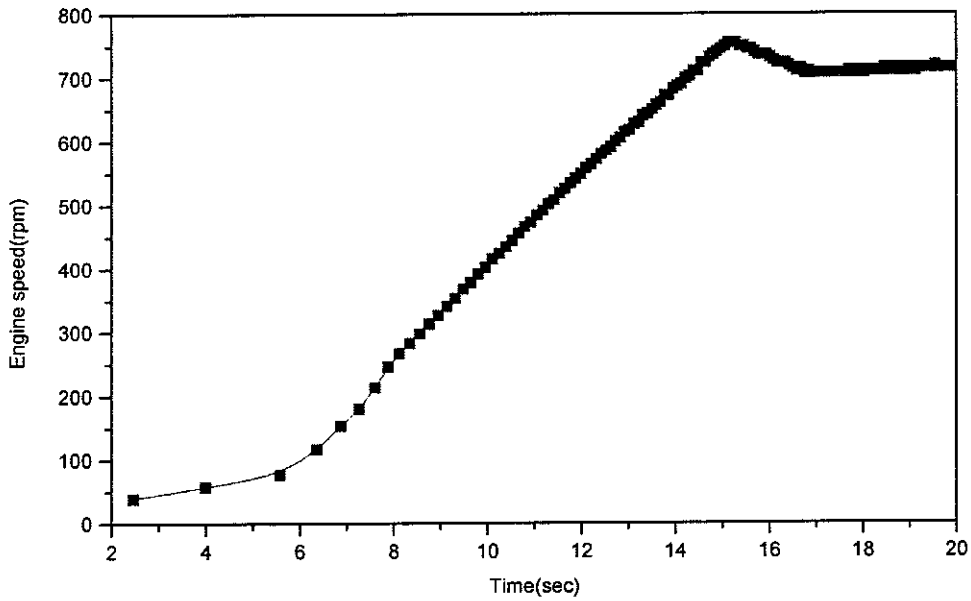

Figure 21. Engine speed-time curve during the run-up of engine with fuel injection

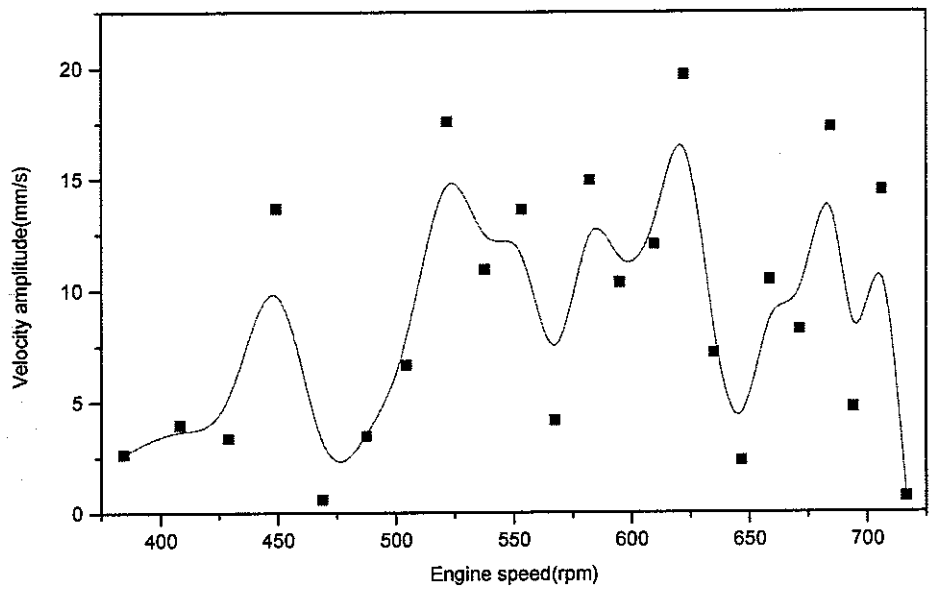

Figure 22. The 1st order velocity amplitude in horizontal-transverse direction of resilient mount right No.1(Measuring point 1) during the run-up of engine

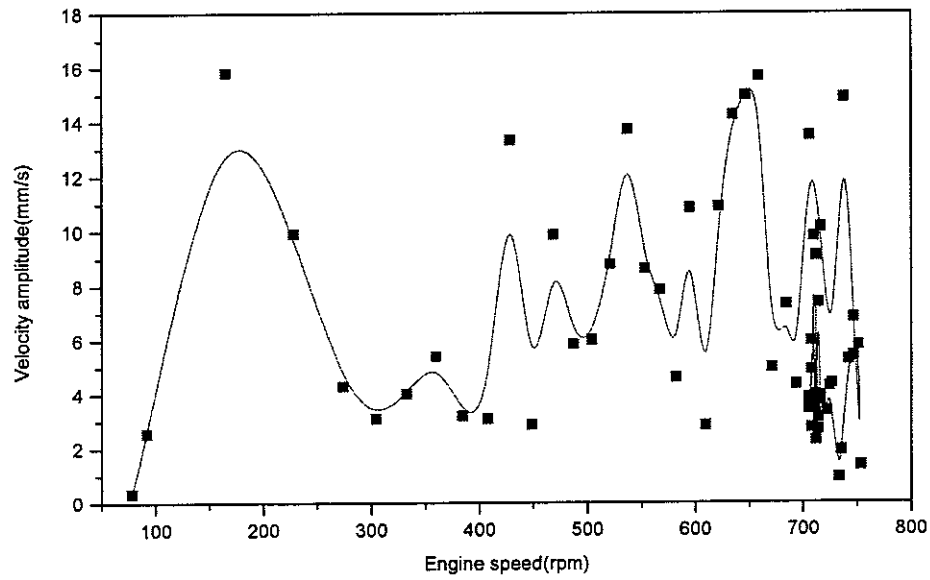

Figure 23. The 1st order velocity amplitude in horizontal-transverse direction of resilient mount right No. 4(Measuring point 2) during the run-up of engine

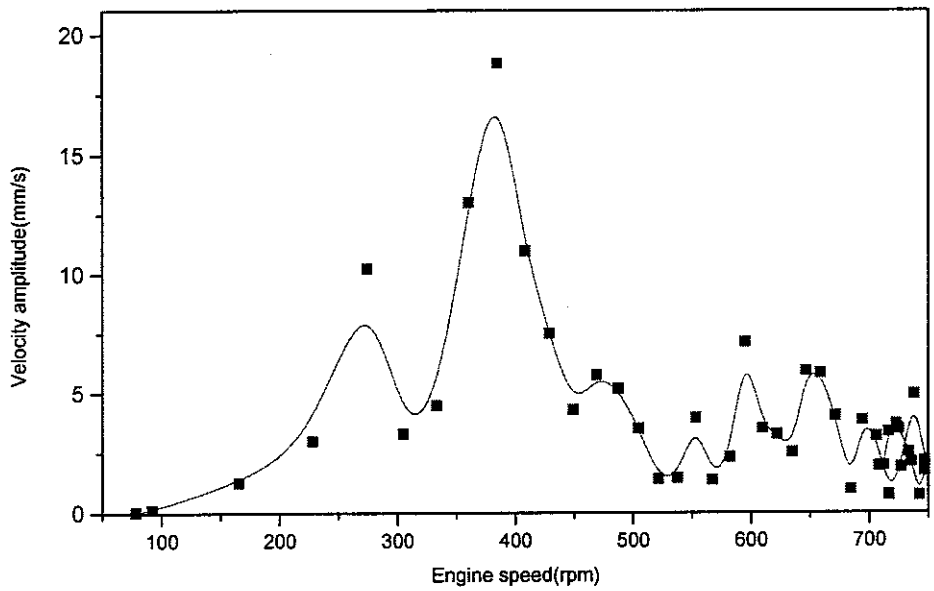

Figure 24. The 4.5th order velocity amplitude in horizontal-transverse direction of resilient mount right No.(Measuring point 1) during the run-up of engine

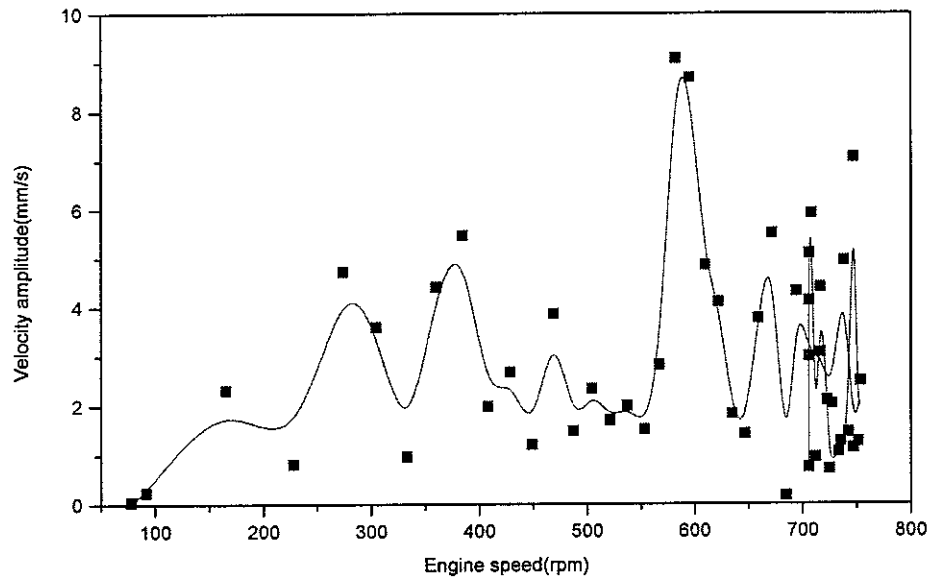

Figure 25. The 4.5th order velocity amplitude in horizontal-transverse direction of resilient mount right No. 4(Measuring point 2) during the run-up of engine

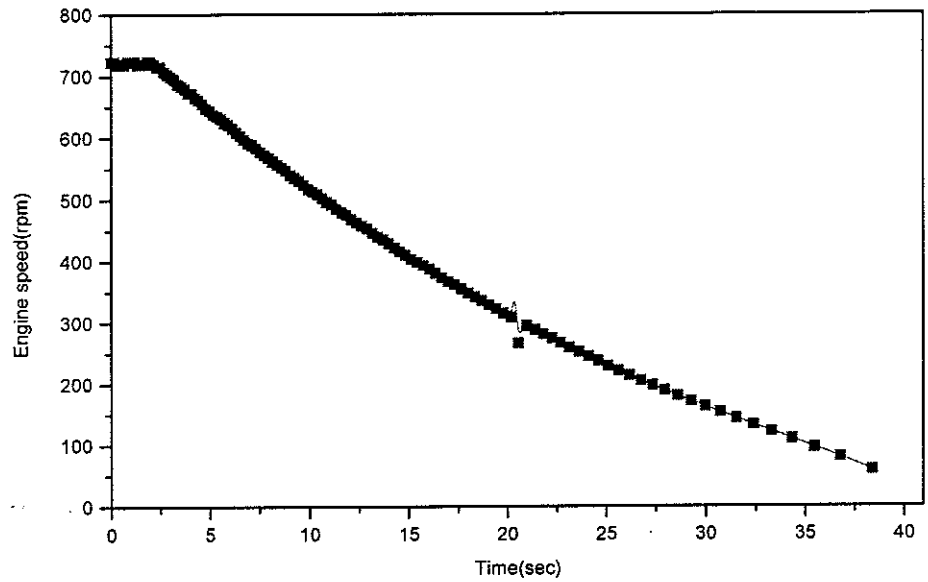

Figure 26. Engine speed-time curve during the run-down of engine with fuel cut-off

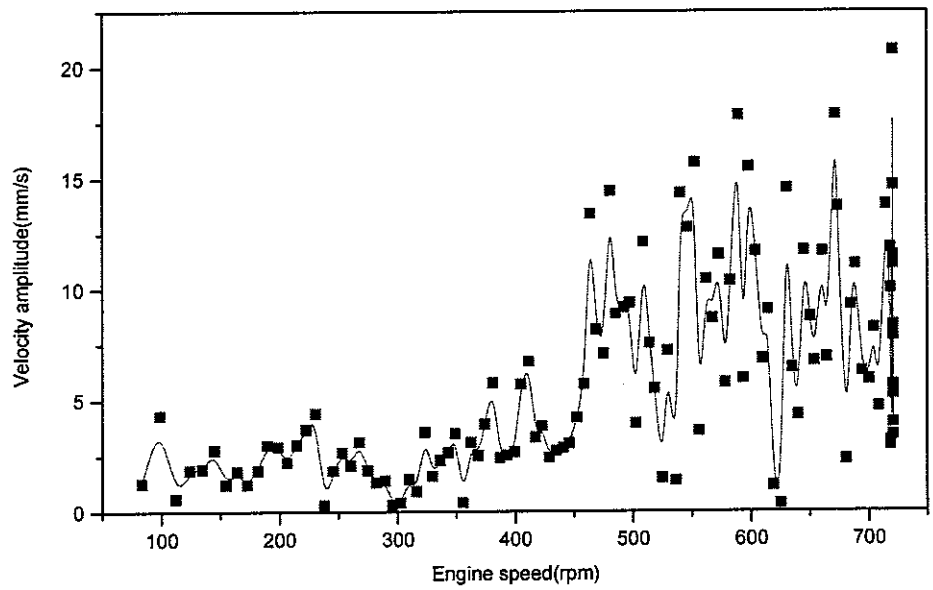

Figure 27. The 1st order velocity amplitude in horizontal-transverse direction of resilient mount right No. 1(Measuring point 1) during the run-down of engine with fuel cut-off

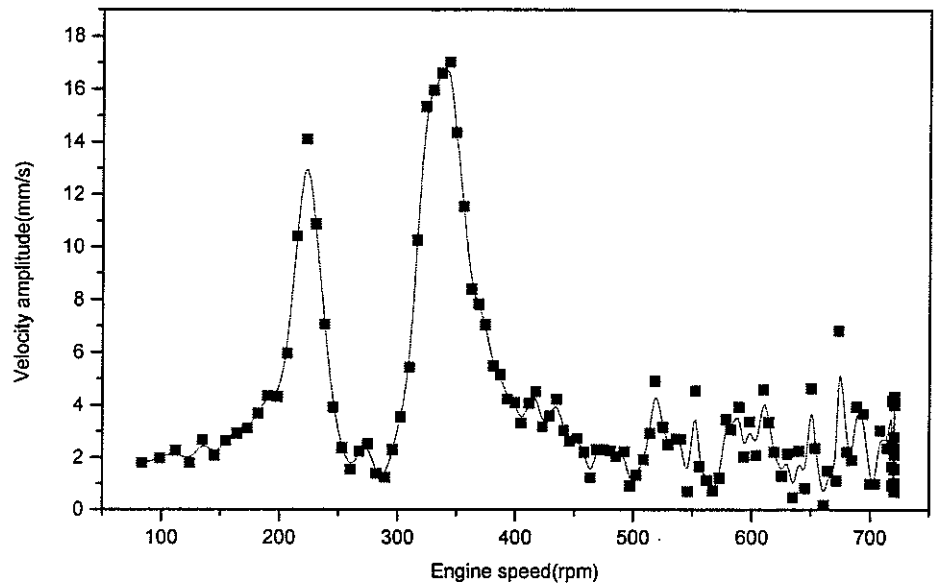

Figure 28. The 4.5th order velocity amplitude in horizontal-transverse direction of resilient mount right No. 1(Measuring point 1) during the run-down of engine with fuel cut-off

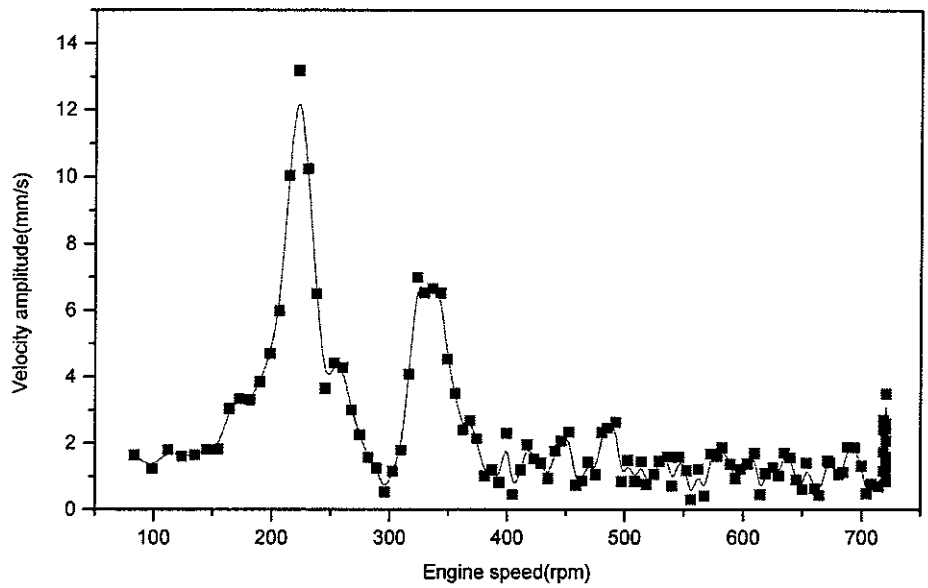

Figure 29. The 4.5th order velocity amplitude in horizontal-transverse direction of resilient mount right No. 4(Measuring point 2) during the run-down of engine with fuel cut-off

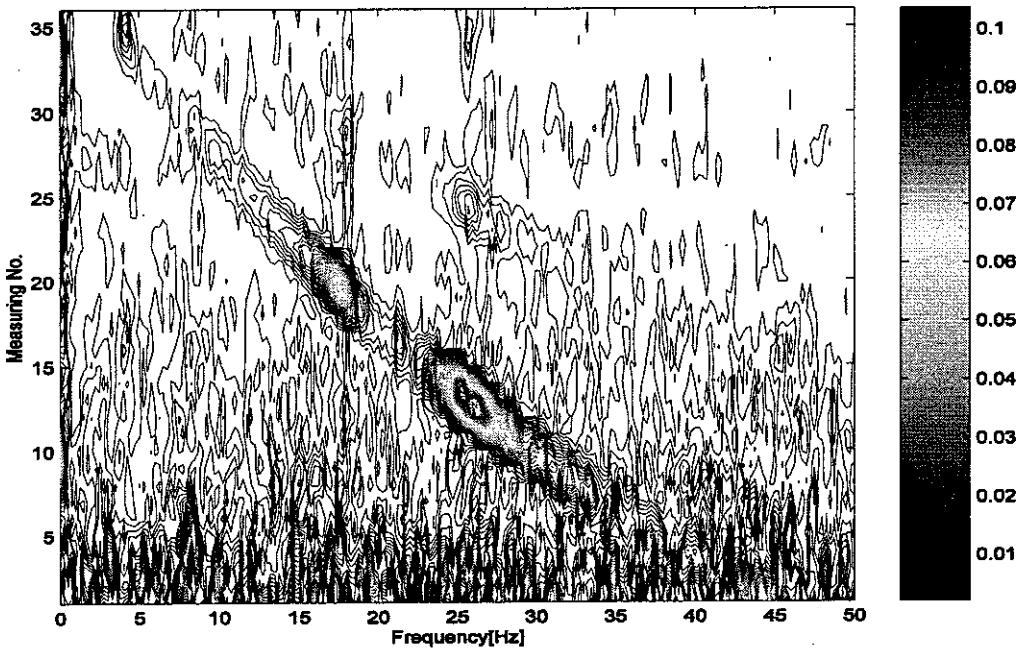

Figure 30. The acceleration amplitude in horizontal-transverse direction of resilient mount right No. 1(Measuring point 1) during the run-down of engine with fuel cut-off engine stopping

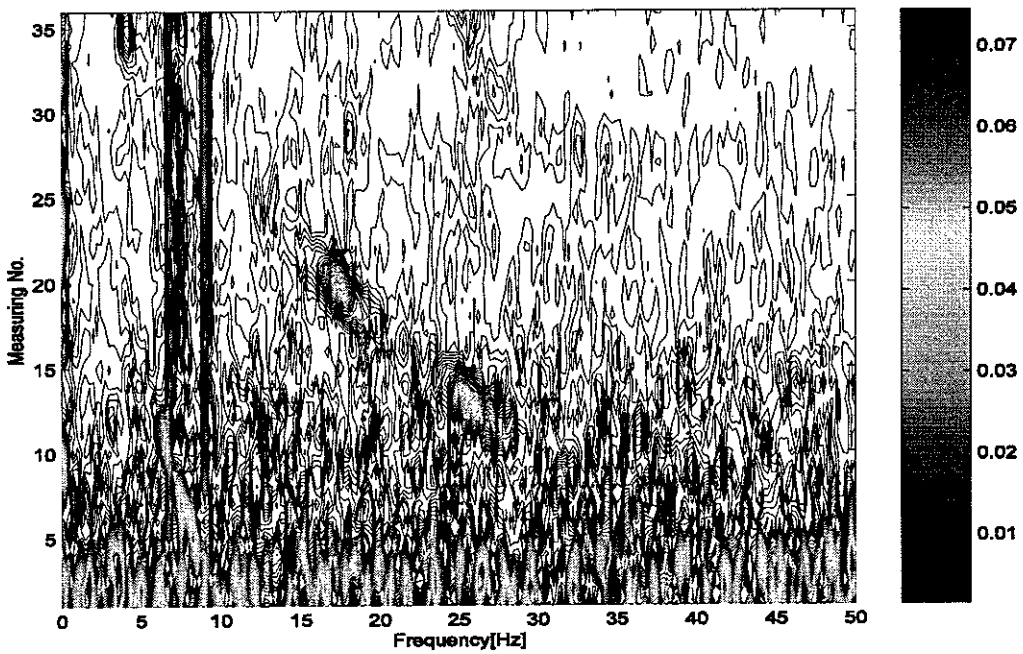

Figure 31. The acceleration amplitude in vertical direction of resilient mount right No. 1(Measuring point 1) during the run-down of engine with fuel cut-off

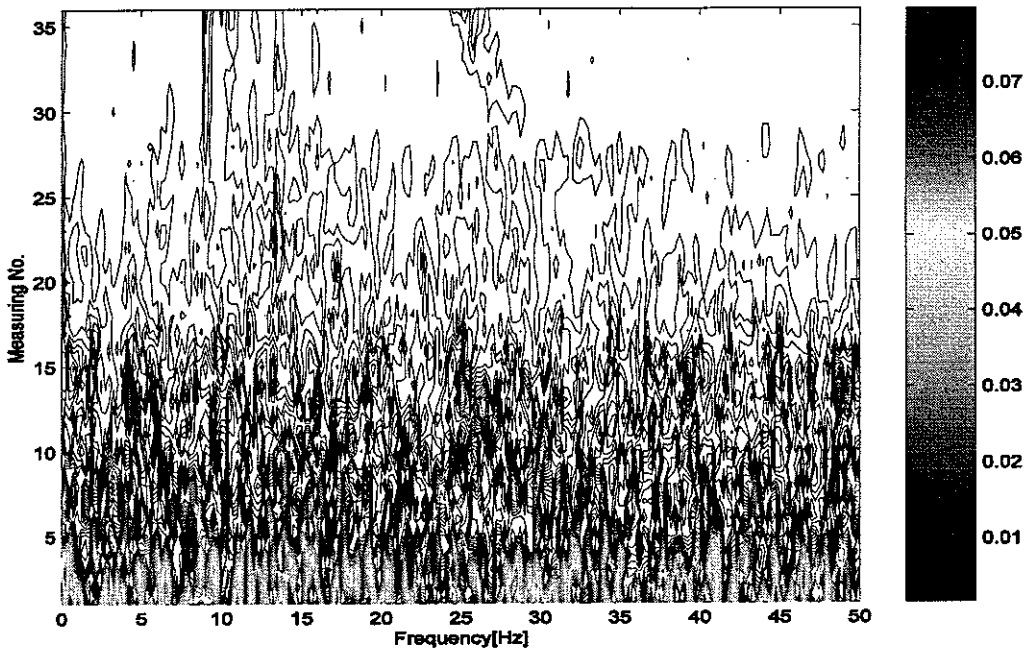

Figure 32. The acceleration amplitude in longitudinal direction of resilient mount right No. 1(Measuring point 1) during the run-down of engine with fuel cut-off

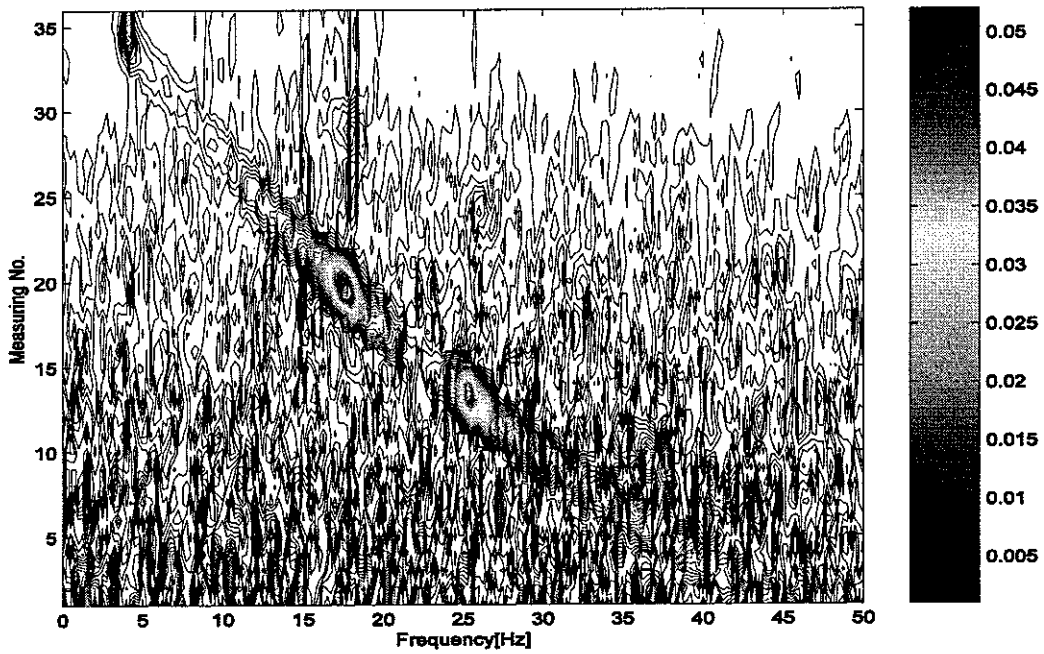

Figure 33. The acceleration amplitude in horizontal-transverse direction of resilient mount right No. 4(Measuring point 2) during the run-down of engine with fuel cut-off

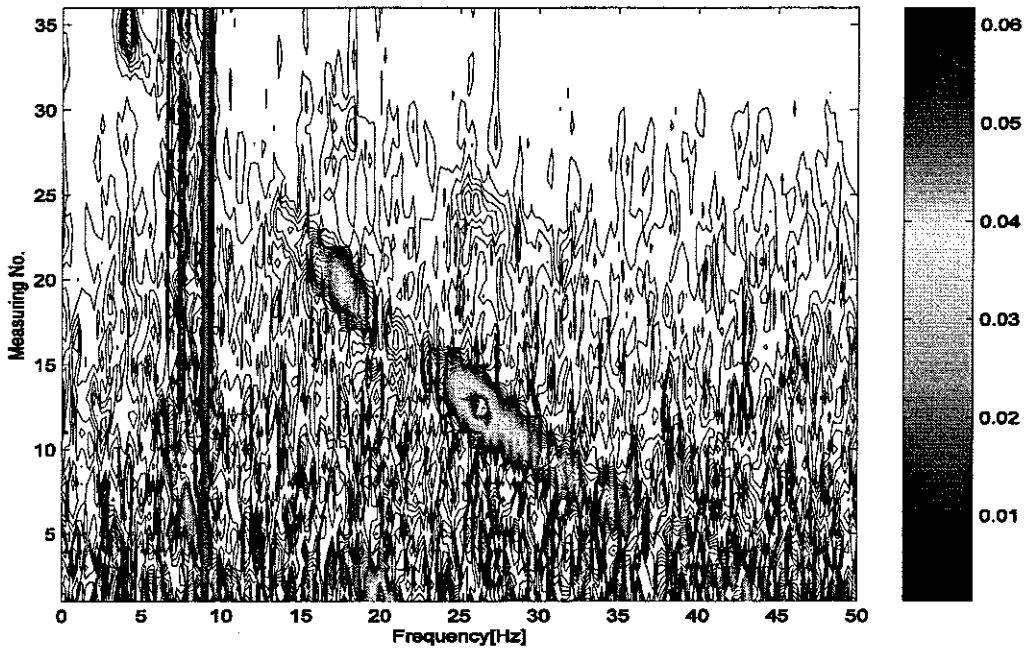

Figure 34. The acceleration amplitude in vertical direction of resilient mount right No. 4(Measuring point 2) during the run-down of engine with fuel cut-off

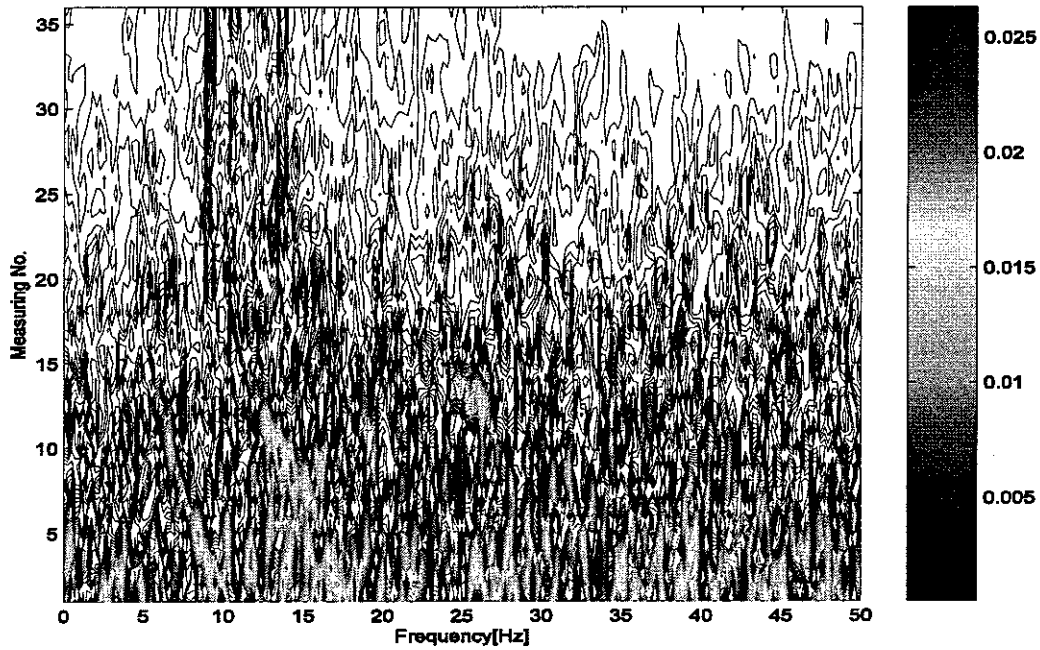

Figure 35. The acceleration amplitude in longitudinal direction of resilient mount number right No. 4(Measuring point 2) during the run-down of engine with fuel cut-off

4.3 Measurement results for mechanical vibration at synchronized speed

The mechanical vibration measured at synchronized speed and at 75% load condition is shown in table 11. Detailed spectra are shown in appendix B figures B1~B24. The engine in rigid body motion excited by torques of 4.5^{th} and 9.0^{th} order, unbalanced torques due to unequaled load of all cylinders and unbalance moments of 1^{st} and 2^{nd} order. However, the transverse vibration of 1.5^{th} order was dominant at the top of the engine and the mounts. The common bed of the test engine, which has a long span of total length 7.36m may be vibrated by an X-type guide force moment like a low speed 2-stroke diesel engine [16]. The X-type guide force moments calculated from tangential harmonic coefficients of this engine are shown in Figure 36. Note that the X-type guide force moment of 1.5^{th} order is larger than other orders. The vibration patterns of other orders (1^{st}, 2^{nd} and 4.5^{th}) are similar to calculated results. The dynamic forces of resilient mounts at 75% load and synchronized speed are shown in table 12. Here the measured dynamic forces were calculated by the displacement amplitudes converted from table 11 and the phase angles of 1^{st}, 1.5^{th}, 2^{nd} and 4.5^{th} amplitudes are assumed as in-phase. The total dynamic forces are 23% greater than the calculated results due to 1.5^{th} order vibration. The square values of velocity amplitudes of the vibration on the top of the resilient mounts for the calculation of the elastic potential energy index at 75% load and 720 rpm are shown in table 13. The total elastic potential energy index at 75% load and synchronized speed is also increase 30.5% greater than the calculated results due to 1.5^{th} order vibration.

Table 11. The velocity amplitudes at 75% load and synchronized speed(unit : mm/s)

Position	Direction	1st order		1.5th order		2nd order		4.5th order	
		Measured	Calculated	Measured	Calculated	Measured	Calculated	Measured	Calculated
Resilient mount right No. 1	x	4.1	4.0	0.4	0.0	1.1	0.3	0.5	0.0
	y	0.9	4.2	5.6	0.7	0.9	0.2	3.2	2.8
	z	4.1	6.1	0.4	0.5	1.0	1.0	0.5	2.2
Resilient mount right No. 4	x	3.6	4.0	0.7	0.0	0.7	0.3	0.4	0.0
	y	0.1	1.0	4.1	0.7	0.8	0.2	2.8	2.8
	z	3.4	1.4	2.0	0.5	1.0	0.2	1.5	2.2
Resilient mount right No. 5	x	4.2	4.0	0.3	0.0	0.8	0.3	0.9	0.0
	y	0.3	1.1	5.2	0.7	0.8	0.2	2.0	2.8
	z	2.2	0.8	1.6	0.5	1.7	0.2	0.6	2.2
Resilient mount right No. 6	x	4.4	4.0	1.0	0.7	0.6	0.3	1.2	0.0
	y	2.1	3.3	0.6	0.7	1.0	0.2	1.4	2.8
	z	6.8	7.1	2.9	0.5	1.7	1.1	0.3	2.2
Engine top-fore (Fuel pump side)	x	6.0	1.1	1.3	0.0	0.7	0.2	0.6	0.0
	y	1.4	3.8	2.1	0.4	2.9	0.1	2.2	2.3
	z	8.0	7.1	2.7	0.4	0.7	1.2	1.8	2.0
Engine top-aft (Fuel pump side)	x	6.3	1.1	0.8	0.0	2.0	0.2	0.3	0.0
	y	0.6	1.5	2.7	0.4	0.3	0.1	1.7	2.2
	z	2.2	2.2	0.8	0.4	1.6	0.4	0.5	2.0

Table 12. The dynamic forces of resilient mounts at 75% load and synchronized speed (unit : N)

Force (direction)	Mount R. No. 1		Mount R. No. 4		Mount R. No. 5		Mount R. No. 6	
	Measured	Calculated	Measured	Calculated	Measured	Calculated	Measured	Calculated
S_x (x)	580	469	523	469	585	469	656	469
S_y (y)	665	594	440	234	536	344	384	497
S_z (z)	478	591	506	173	381	421	876	687
S_s (Synthesis)	1004	962	856	524	880	718	1160	963

Table 13. The square value of velocity amplitude of resilient mounts at 75% load and synchronized speed (unit : mm^2/s^2)

Square velocity (direction)	Mount R. No. 1		Mount R. No. 4		Mount R. No. 5		Mount R. No. 6		Summation	
	Measured	Calculated	Measured	Calculated	Measured	Calculated	Measured	Calculated	Measured	Calculated
$\sum v_x^2$ (x)	18.4	16.1	14.1	16.1	19.2	16.1	22.2	16.9	73.9	65.2
$\sum v_y^2$ (y)	30.0	26.0	25.3	9.4	31.8	9.6	10.6	7.3	97.7	52.3
$\sum v_z^2$ (z)	18.2	43.3	18.8	7.1	10.7	5.8	75.0	56.3	122.7	112.5

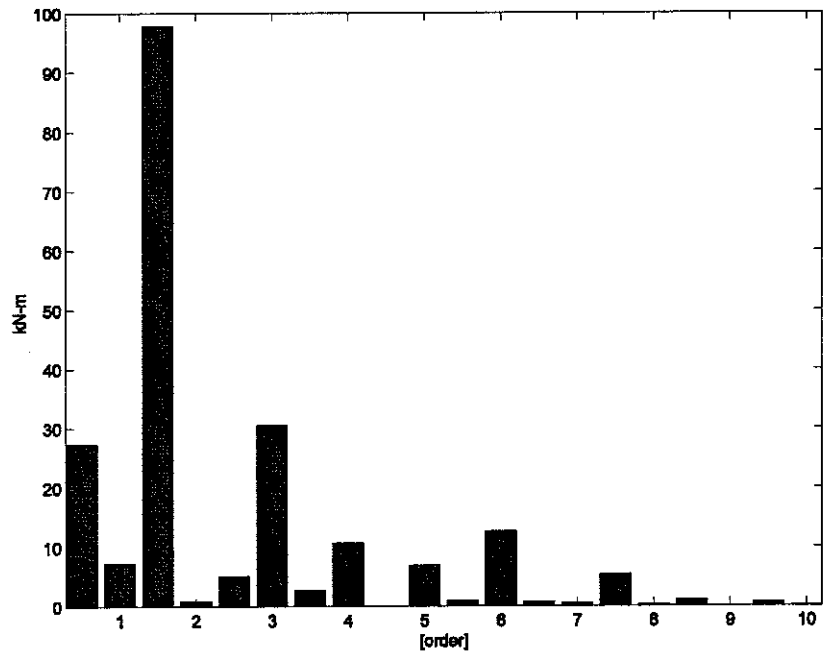

Figure 36. X-type guide force moments of 9L28/32 generator engine at full load and synchronized speed(720 rpm)

4.4 Measurement result for structure-borne noise at synchronized speed

The structure-borne noise in the x, y, z directions of the resilient mount(shown in figure 37) upper part(engine side) and resilient mount lower part(hull side) is was measured at synchronous speed and at 75 % generator load condition. The results of one-third octave band which were

measured using CIMAC(International council on combustion engines)'s recommendation [19] are shown in table 14 and Appendix C figures C1~C24. As the results show, the vibration reduction effects of resilient mounts are satisfactory for the transverse and longitudinal directions. However its effect in the vertical direction is not good due to the flexibility of hull structure. In particular the structure-borne noise level in the vertical direction between 100 and 250 Hz was increased by the vertical resonance of the engine foundation.

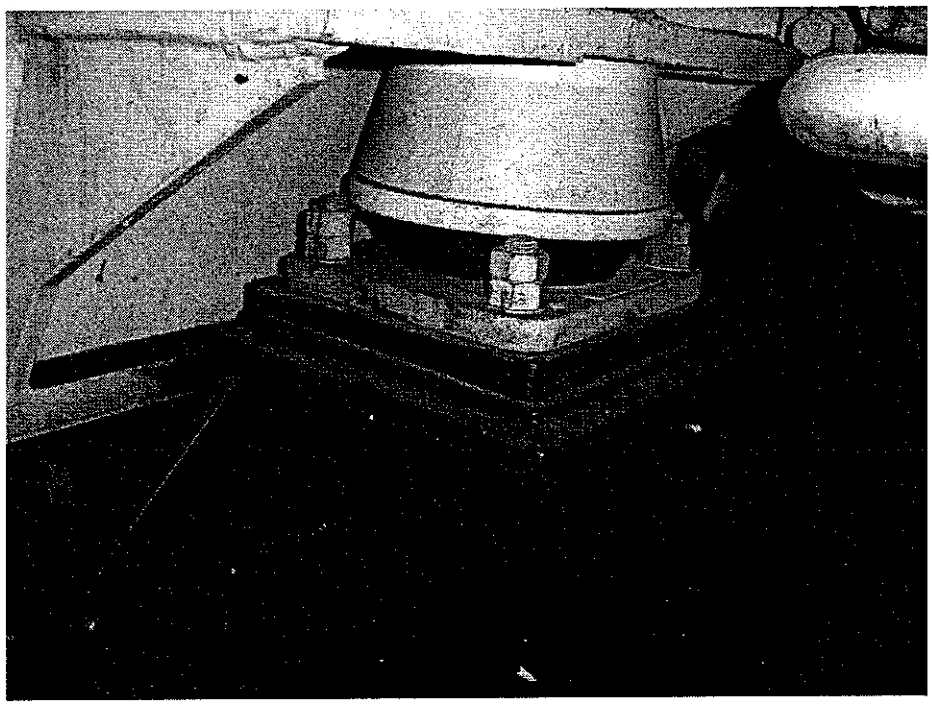

Figure 37 Picture of resilient mount

Table 14(a) Overall level and transmission loss for structure-borne noise on the resilient mounts (Unit : dB ref.10^{-9} m/s)

Position	Direction	Engine Side(A)	Hull side(B)	Reduction (A-B)	1/3 Octave band spectrum No. (Appendix C)
Mount right No. 1	*x* (Longitudinal)	129.1	110.5	18.6	Fig. C1 and C2
	y (Transverse)	133.4	121.8	11.7	Fig. C3 and C4
	z (Vertical)	132.9	120.5	12.4	Fig. C5 and C6
Mount right No. 4	*x* (Longitudinal)	127.1	106.9	20.2	Fig. C7 and C8
	y (Transverse)	132.8	121.6	11.2	Fig. C9 and C10
	z (Vertical)	135.8	122.3	13.5	Fig. C11 and C12
Mount right No. 5	*x* (Longitudinal)	126.8	108.5	18.3	Fig. C13 and C14
	y (Transverse)	129.8	123.6	6.2	Fig. C15 and C16
	z (Vertical)	131.8	125.2	6.6	Fig. C17 and C18
Mount right No. 6	*x* (Longitudinal)	126.6	110.2	16.4	Fig. C19 and C20
	y (Transverse)	131.3	119.3	12.0	Fig. C21 and C22
	z (Vertical)	131.4	121.1	10.2	Fig. C23 and C24

Table 14(b) Level and transmission loss between 100 Hz and 250 Hz for structure-borne noise on the resilient mounts (Unit : dB ref.10^{-9} m/s)

Position	Direction	Engine Side(A)	Hull side(B)	Reduction (A-B)	1/3 Octave band spectrum No. (Appendix C)
Mount right No. 1	*x* (Longitudinal)	118.4	101.9	16.5	Fig. C1 and C2
	y (Transverse)	123.7	117.6	6.1	Fig. C3 and C4
	z (Vertical)	122.1	117.3	4.8	Fig. C5 and C6
Mount right No. 4	*x* (Longitudinal)	112.6	93.7	18.9	Fig. C7 and C8
	y (Transverse)	119.1	115.6	3.5	Fig. C9 and C10
	z (Vertical)	119.9	115.8	4.1	Fig. C11 and C12
Mount right No. 5	*x* (Longitudinal)	114.4	94.3	20.1	Fig. C13 and C14
	y (Transverse)	117.9	120.4	-2.5	Fig. C15 and C16
	z (Vertical)	113.6	117.7	-4.1	Fig. C17 and C18
Mount right No. 6	*x* (Longitudinal)	117.4	102.3	14.9	Fig. C19 and C20
	y (Transverse)	115.9	114.3	1.6	Fig. C21 and C22
	z (Vertical)	113.5	114.8	-1.3	Fig. C23 and C24

5. CONCLUSIONS

The dynamic behaviour and transmission of structure-borne noise of a marine diesel engine generator supported using resilient mounts on a 5500 TUE container vessel have been investigated in this report. A theoretical analysis of this installation was performed by using a 6 degree of freedom simplified rigid body installation. Actual measurements of mechanical vibration of engine and structure-bone noise of the engine foundation on board were carried out to verify these. The main findings can be summarized as follows.

1) The calculated natural frequencies of a one-mass-6-degree freedom simplified rigid body model, excluding the elastic effect of engine foundation correspond reasonably well with the measured results. However the 1.5^{th} order flexible twisting vibration mode of the common bed by twisting was unexpectedly measured and its forced response was dominant at synchronized speed of 720 rpm. So, the flexible mode of vibration of a common bed of a marine diesel engine generator, unlike the propulsion engine should be carefully investigated in the design stage.
2) The design criteria for a marine diesel engine generator may only be approximately specified in terms of the magnitude of mechanical vibration of the engine. However, this method is not satisfactory for a marine diesel engine generator with a resilient mount system. A new approach has been proposed which is to estimate the total dynamic force transmitted to the supporting structure and potential elastic energy index stored in the resilient mounts.
3) If the vertical vibration resonances of the engine foundation coincide with the rotational modes of 0.5^{th}, 1^{st}, 1.5^{th} ... times the excitation of the cylinder number at the synchronous speed of the generator, the structure-borne noise transmitted to the engine foundation may rapidly increase. As a countermeasure, these resonances should be avoided by the modifying the engine's foundation or changing the numbers of engine cylinders.

References

1. TNO-report 1994 TPD-HAG-PRT-940167-RD, Noise and vibration isolation with mountings : how many, how stiff.

2. J. Jenser, Technical report of Wärtsilä NSD 1997, Vibration aspects.

3. Wärtsilä 2003, Technology review for Wärtsilä 46.

4. T. J. Royston and R. Singh 1996 *Journal of Sound and Vibration* 194, 295-316. Optimization of passive and active non-linear vibration mounting systems based on vibration power transmission.

5. D. H. Lee, W. S. Hwang and C. M. Kim 2002 *Journal of Sound and Vibration* 255, 383-397. Design sensitivity analysis and optimization of an engine mount system using an FRF-based sub structuring method.

6. J. S. Tao, G. R. Liu and K. Y. Lam 2000 *Journal of Sound and Vibration* 235, 477-497. Design optimization of marine engine-mount system.

7. J. H. Kim and J. M. Lee 2000 *Institution of Mechanical Engineers* D04098, 45-53. Elastic foundation effects on the dynamic response of engine mount systems.

8. P. Bonello and M. J. Brennan 2001 *Journal of Sound and Vibration* 239, 445-466. Modelling the dynamic behaviour of a supercritical rotor on a flexible foundation using the mechanical impedance technique.

9. ISO 10846-1 1997(E), Acoustics and vibration-Laboratory measurement of vibro-acoustic transfer properties of resilient elements part 1: Principles and guidelines.

10. ISO 10846-2 1997(E), Acoustics and vibration-Laboratory measurement of vibro-acoustic transfer properties of resilient elements part 2: Dynamic stiffness of elastic supports for translatory motion (Direct method).

11. ISO 10846-3 2002(E), Acoustics and vibration-Laboratory measurement of vibro-acoustic

transfer properties of resilient elements part 2: Dynamic stiffness of elastic supports for translatory motion (Indirect method).

12. Rubber design Co., Marine mountings catalog, 2004.

13. Nuno M. M. Maia and Julio M. M. Silva, Theoretical and experimental modal analysis, Research studies press ltd., 1996.

14. A. N. Thite and D. J. Thompson 2003 *Journal of Sound and Vibration* 264, 411-431. The quantification of structure-borne transmission paths by inverse methods. Part 1: Improved singular value rejection method.

15. Cyril M. Harris, Shock and vibration handbook, 3rd edition, McGraw-Hill, New York, 1986.

16. D. C. Lee, Y. K. Kim, U. K. Kim and H. J. Jeon 1998 *22nd CIMAC(International council on combustion engines) World Congress 1998 Copenhagen*, 1635-1648. A Study on the Vibration Controls for the Diesel Power Plant with Paralleled Two Stroke Low Speed Diesel Engines.

17. ISO 8528-9 1991, Reciprocating internal combustion engine driven alternating current generating sets- Part 9 : Measurement and evaluation of mechanical vibrations.

18. Wärtsilä 2004, Marine news N0.2-2004/Guidelines to engine dynamics and vibration.

19. CIMAC(International council on combustion engines) 1994 Number 14 Standard method for the determination of the structure-borne noise from engines